Basolateral amygdala dopamine transmits a nonassociative emotional salience signal

Megan A. Brickner[1,2,3], William E. Szot[1,2], Amy R. Wolff, PhD[1,2], Mark J. Thomas, PhD[1,2], Benjamin T. Saunders PhD[1,2]

[1] Department of Neuroscience, University of Minnesota
[2] Medical Discovery Team on Addiction, University of Minnesota
[3] Graduate Program in Neuroscience, University of Minnesota

Correspondence: BTS (bts@umn.edu, saunderslab.com)

PREPRINT

Adaptive decision making relies on proper discrimination and prediction of positive and negative events. The basolateral amygdala (BLA) is central to this valence encoding, assigning emotional value to stimuli to drive appropriate behavioral responses. The ventral tegmental area (VTA), which is classically known to regulate associative learning and incentive motivation via dopamine projections to the striatum, also contains strong dopamine projections to the BLA, but this system has received much less attention. Here, we investigated how *in vivo* BLA dopamine signaling is engaged durning learning. We show that reward cues evoke BLA dopamine signals that diminish, rather than grow, with training. As the complexity of the learning context was increased, where rats actively differentiated between various cue types signaling threat, reward, safety, and neutral associations, the magnitude of cue-evoked BLA dopamine responses was largest early in training and reported the level of perceived emotional saliency. Fear and safety cues prompted larger, sustained dopamine signals compared to reward and neutral cues, an effect that was more apparent in female rats, compared to males. Together, our findings broaden the theoretical landscape of dopamine heterogeneity, showing that BLA dopamine supports dynamic disambiguation of relative stimulus importance by non-associatively encoding sensory state transitions, independent of value. These signals reflect a scalar readout of emotional salience to prime, rather than track, learning.

INTRODUCTION

An underlying foundation of behavior is the associative learning that cements relationships between environmental cues and the biologically relevant outcomes they predict. Differential encoding of positive and negative valenced sensory inputs is then imperative for directing appropriate decision making. The basolateral amygdala (BLA) is a key brain structure in this process, integrating sensory information from multiple brain regions and assigning emotional value to cues and environmental contexts (O'Neill et al. 2018; Paton et al. 2006). The BLA is central to fear (Duvarci & Pare 2014; Maren 2005) as well as reward learning (Cador et al. 1989; Everitt et al. 1991; Ottenheimer et al. 2024; Sias et al. 2021; Whitelaw et al. 1996), and is involved in discrimination learning of both fear and reward responses (Duvarci & Pare 2014; Janak & Tye 2015; Ng et al. 2018; Sangha 2015; Sangha et al. 2013, 2020; Sias et al. 2024) via dynamic valence encoding (Rogan et al. 2005; Sangha et al. 2013; Sengupta et al. 2018; Tye et al. 2008).

The BLA's role in emotional learning is partly driven by excitatory inputs from cortex, thalamus and other regions, but the contribution of neuromodulatory circuit inputs is less clear (Beyeler et al. 2018; Khalil et al. 2023; Leppla et al. 2023; Li et al. 2025; McGarry & Carter 2017; Namburi et al. 2015; O'Neill et al. 2018; Paton et al. 2006; Saddoris et al. 2005). Notably, dopamine neurons in the ventral tegmental area (VTA), which are classically known to regulate reward learning and incentive motivation via projections to the striatum (Fields et al. 2007; Yang et al. 2018) also contain dense

projections to the BLA (Brinley-Reed & McDonald 1999; Lutas et al. 2019; Mingote et al. 2015; Takahashi et al. 2010), but this system has received much less attention. On slow timescales, amygdala dopamine levels increase as rats learn to distinguish between states where food is or is not available in the environment (Hori et al. 1993). Recent studies offer more insights, showing that dopaminergic VTA-BLA axons are rapidly activated during rewards and punishments (Correia & Goosens 2016; Lutas et al. 2019, 2022; Sias et al. 2024; Tang et al. 2020) and respond to predictive cues (Correia & Goosens 2016; Lutas et al. 2019; Sias et al. 2024; Tang et al. 2020). Further, BLA dopamine signaling encodes information relating to reward-identity memories (Correia & Goosens 2016; Lutas et al. 2019; Sias et al. 2024; Tang et al. 2020). Despite this growing focus, we still know very little about how the BLA dopamine system is engaged during learning. Delineating this aspect of heterogeneity is critical as part of evolving complexities of the role of dopamine in valuation and

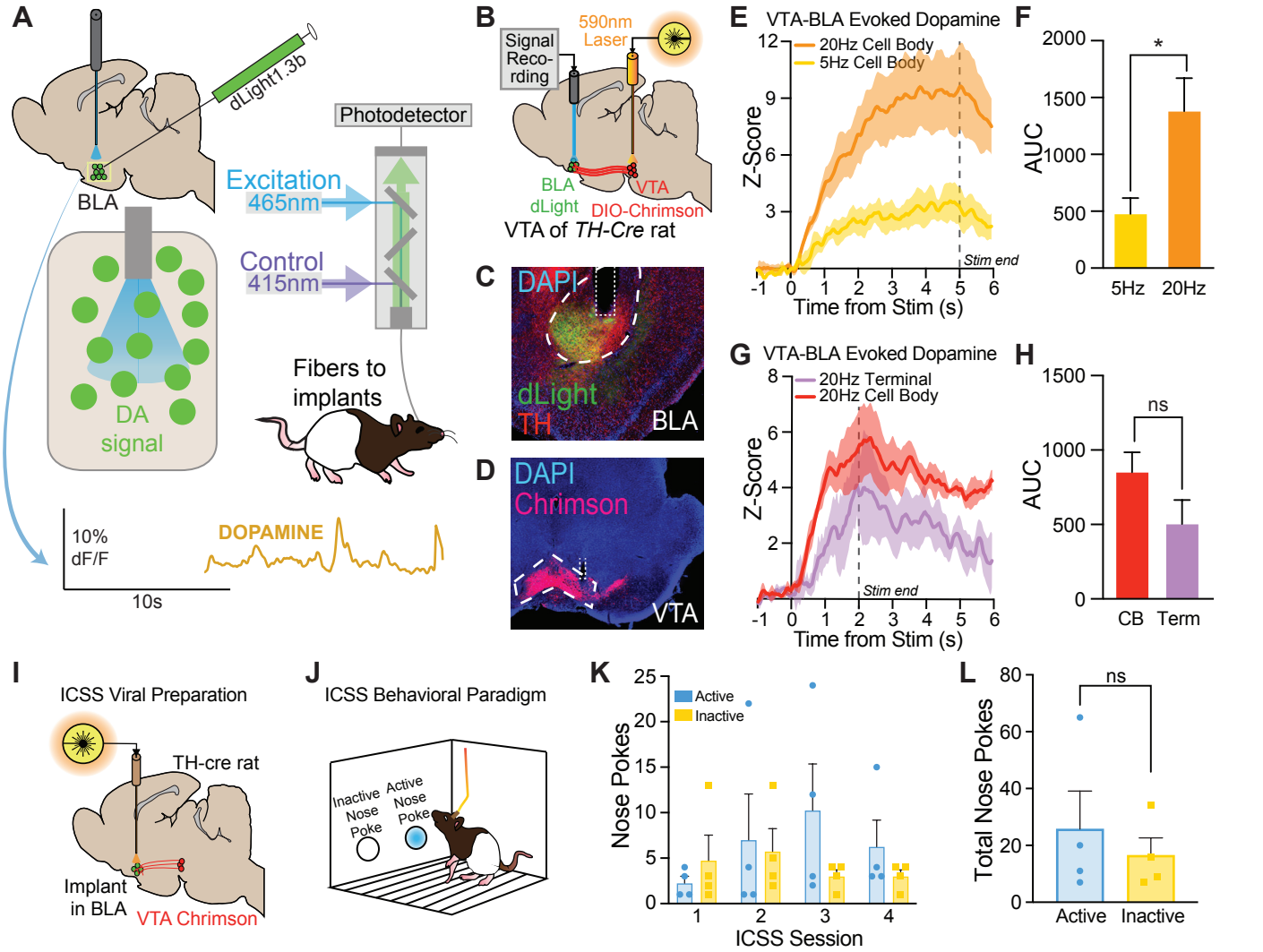

Fig 1 | Optogenetic activation of VTA dopamine neurons evokes robust dopamine signaling in the BLA that does not support reinforcement

A) Schematic of the photometry system to record BLA dopamine dynamics. B) Viral approach for simultaneous in vivo optogenetic activation VTA dopamine neuron cell bodies or terminals in the BLA paired with fiber photometry recording of dopamine transmission in the BLA. Dopamine neurons were targeted in TH-cre transgenic rats with DIO-Chrimson opsin (n=3). C) Example of dLight1.3b viral expression in the BLA, with tissue counterstained for visualization of overlapping tyrosine hydroxylase (TH). D) Example of DIO-Chrimson expression in VTA dopamine neurons. E, F) Optogenetic excitation of VTA dopamine cell bodies resulted in frequency-dependent dopamine release in the BLA, where 5 s stimulation at 20Hz prompted a larger response compared to 5 s stimulation at 5Hz. G, H) Optogenetic excitation of VTA dopamine neuron terminals in the BLA also resulted in robust BLA dopamine release, which was comparable to the signal evoked by cell body stimulation for 2 s at 20Hz. I) Viral approach for intracranial self stimulation (ICSS) of VTA-BLA dopamine terminals using DIO-Chrimson infused in the VTA of TH-cre rats and optic fibers implanted over the BLA. J) Schematic of the ICSS behavioral paradigm, where rats could nose poke to activate VTA-BLA dopamine terminals to prompt dopamine transmission into the BLA. K) Rats (n=4) did not readily poke for BLA dopamine terminal activation during ICSS, making the same number of active nose pokes (ANPs) and inactive nose pokes (INPs). L) Total number of ANPs and INPs during ICSS collapsed across sessions. AUC = Area under curve. Data represent mean ± SEM. *p<0.05.

salience encoding (Bornhoft et al. 2025; Kutlu et al. 2021; Lammel et al. 2014; McCutcheon et al. 2012; van Elzelingen et al. 2022a,b).

To investigate this, we used fiber photometry to characterize *in vivo* BLA dopamine signals as rats engaged in various learning tasks. We first show that appetitive and aversive stimuli independently evoke strong positive dopamine responses in the BLA, and reward-cue evoked responses diminish, rather than grow, with training. We then tracked the emergence of *in vivo* BLA dopamine in response to four differently valenced cue types during a Pavlovian cue discrimination task. In this more complex learning context, where cues signaling threat, reward, safety, and neutral associations were intermingled within a session, we found that the magnitude of cue-evoked BLA dopamine responses scaled with perceived emotional saliency: fear and safety cues evoked strong signals early in conditioning that were larger than for reward and neutral cues, and these signals were resistant to extinction. Notably, we found a consistent sex bias in BLA dopamine signals, where female rats had stronger and more threat biased dopamine signaling, compared to males. In additional studies, we demonstrate optogenetic stimulation of dopamine release in the BLA does not directly drive learning via reinforcement. Together, our data support the conclusion that BLA dopamine signals provide a unique contribution to emotional learning compared to classic striatal systems by non-associatively encoding sensory state transitions, independent of value. This state-guided saliency signal is dynamically engaged in a learning context where relative stimulus importance must be disambiguated.

RESULTS

Optogenetic activation of VTA-BLA dopamine neurons evokes strong BLA dopamine release but does not support reinforcement

To record amygdala dopamine signaling in freely behaving rats, we used fiber photometry with the dLight1.3b sensor (**Fig 1A**). First, to validate this approach and determine how VTA TH-neuron stimulation influences dopamine dynamics in the BLA, a cre-driven Chrimson opsin was expressed into the VTA of TH-cre rats to specifically target the dopamine neurons (**Fig 1B,D**), while dLight1.3b was expressed in the ipsilateral BLA (**Fig 1B,C; Fig S1**). Optogenetic activation of VTA dopamine neurons via 590-nm laser pulses evoked robust dopamine signals in the BLA, which positively scaled with stimulation frequency (**Fig 1E,F**; $t(2)=4.919$, $p=0.0389$). We next targeted optogenetic activation to VTA dopamine terminals in the BLA to confirm locally evoked dopamine release. Terminal stimulation also resulted in robust dopamine signaling (**Fig 1G**) that was comparable to that evoked by brief dopamine cell body stimulation (**Fig 1H**; $t(2)=1.271$, $p=0.3315$).

VTA dopamine projections to the striatum are known to support behavioral reinforcement (Kim et al. 2012; Steinberg et al. 2014; Witten et al. 2011; Wolff & Saunders 2024). Given the strong evoked dopamine signal we observed in the BLA, we next tested whether VTA-BLA dopamine transmission also promotes reinforcement (**Fig 1I**). Rats were given the opportunity to nose poke for optogenetic activation of VTA dopamine terminals in the BLA, in an Intracranial Self Stimulation (ICSS) procedure (**Fig 1J**). Overall, rats did not readily nose poke for stimulation (**Fig 1K**; $F(1,3)=1.257$, $p=0.3439$), and active nose pokes were not significantly different from inactive nose pokes during training (**Fig 1L**; $t(3)=1.121$, $p=0.3439$).

In vivo BLA dopamine signals respond to valenced events

We next recorded BLA dopamine dynamics in response to differently valenced unconditioned stimuli - sucrose consumption and footshock. Rats were first given the opportunity to drink sucrose, delivered into a magazine port, which prompted a moderate increase in dopamine (**Fig 2A**). Delivery of moderate (0.5mA, 0.5s) footshocks elicited a strong phasic increase in dopamine (**Fig 2B**). Comparing the signals directly, footshock-evoked signals were significantly larger than sucrose evoked signals (**Fig 2C**; $t(12)=2.595$, $p=0.0234$). Broadly, these results show that both positive and negative events prompt positive release of BLA dopamine, with a bias of stronger responses for aversive stimuli.

Simple reward conditioning promotes diminishing cue-evoked BLA dopamine signals across training

To explore how BLA dopamine dynamics track associative learning and valence discrimination, rats were prepared for BLA dopamine photometry and then trained on a multi-phase Pavlovian cue discrimination paradigm adapted from previous studies (Sangha et al. 2013; **Fig 3A**). Rats first underwent reward-only conditioning, followed by a compound reward and fear conditioning phase. This was then followed by the full cue discrimination task, where rats had to distinguish between four different, interleaved Pavlovian cue associations - reward, fear, safety, and neutral. Finally, reward and fear cues underwent extinction (**Fig 3A**). Throughout this, we measured two main conditioned responses: sucrose port entries and freezing, which were similar across males and females (**Fig S2**). However, in our initial assessment of

the photometry data, we saw strong sex-related biases in BLA dopamine signals, and qualitatively different patterns of activity (**Fig S3**), in various task phases. As a result, we split the photometry data by sex to clearly illustrate those patterns.

In the simple reward conditioning phase, an auditory cue predicted sucrose reward delivery (**Fig 3D**). Rats learned this association quickly and increased their sucrose port entry behaviors across training (**Fig 3B**; $F(6,87)=6.14$, $p<0.0001$), while conditioned freezing behaviors were minimal (**Fig 3C**; $F(2, 45)=0.24$, $p=0.79$). Females and males responded with similar levels of locomotion and port entry behavior during reward conditioning (**Fig S2**). Reward cue presentations evoked dopamine increases on all days of training in both females (**Fig 3E**) and males, (**Fig 3G**). Notably, in females, cue-evoked dopamine was the greatest on the first day of conditioning and decreased significantly as reward conditioning progressed **(Fig 3F**; $F(2,16)=7.438$, $p=0.0052$; post hoc comparisons for session 4 vs 1, $p=0.0166$; session 7 vs 1, $p=0.0077$). Cue-evoked peaks were lower overall in males, but a similar pattern emerged, where the reward cue evoked diminishing dopamine across training (**Fig 3H**; $F(2,12)=4.105$, $p=0.0438$).

Sex-biased BLA dopamine responses to intermingled, differentially valenced Pavlovian cues

Following simple reward conditioning, an auditory cue predicting footshock was added, interleaved with reward cue trials in a compound conditioning session (**Fig 3I**). On this session, rats maintained their sucrose port entry behaviors during the reward cue and spent significantly more time in the sucrose port during the reward cue compared to the fear cue (**Fig 3B**; $t(8)=4.671$, $p=0.0016$). Freezing behavior rapidly emerged to the fear cue but not the reward cue (**Fig 3C**; $t(8)=3.905$, $p=0.0045$), and reward cue freezing did not differ from simple reward conditioning (**Fig 3C**; $t(8)=0.1993$, $p=0.8470$). This indicates rats were able to behaviorally discriminate the cues during compound conditioning, with similar levels of conditioned behaviors and cued locomotion between females and males (**Fig S2**).

We examined the BLA dopamine signals on this session, when both reward and fear learning were engaged. In females, the fear cue elicited a large, sustained dopamine peak that was significantly larger than the reward cue signal (**Fig 3J,K**; $t(4)=2.835$, $p=0.0471$), which had a moderate peak before returning to baseline. Notably, on this compound conditioning session, the reward cue evoked dopamine signal rebounded relative to the final day of simple reward conditioning (**Fig 3E,J)**, returning to the same magnitude it showed during the first day of reward conditioning (**Fig 3F,K**; $t(4)=1.509$, $p=0.2059$). In contrast, fear and reward cue dopamine signals were similar in males (**Fig 3L,M**; $t(3)=1.354$, $p=0.2688$), with moderate peaks and a relatively quick return to baseline (**Fig 3L**). Further, the male reward cue signal stayed dampened even with the fear cue added into training, similar to values seen in later reward conditioning training (**Fig 3H,M**; $t(3)=0.6938$, $p=0.5377$).

Rats discriminate fear, safety, and reward predictive cues

Previous in vivo single unit recordings have demonstrated that a population of BLA neurons become responsive during cue discrimination training, including to a safe-

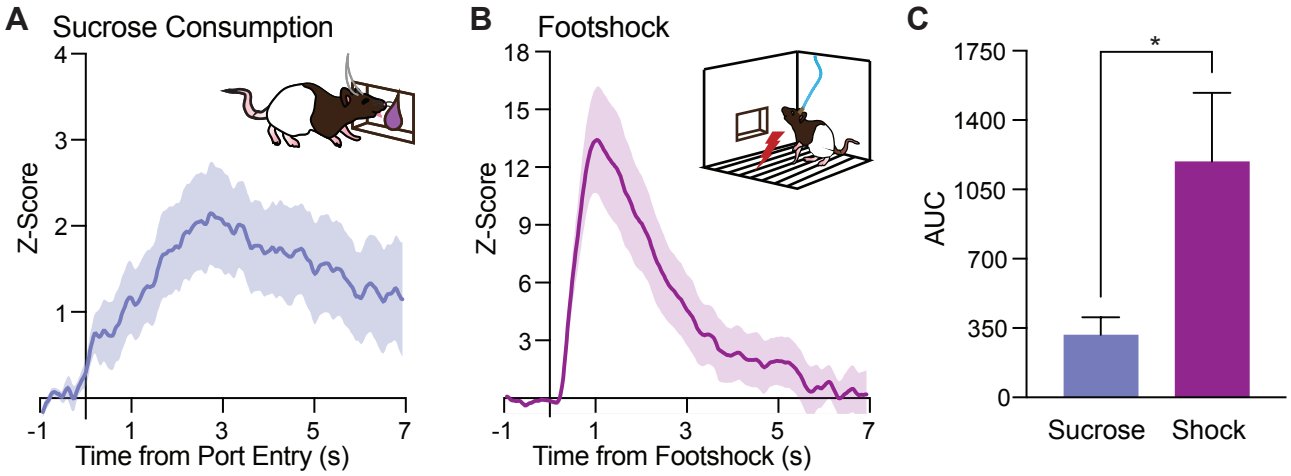

Fig 2 | Appetitive and aversive stimuli engage different BLA dopamine dynamics

A) Rats (n=16) were given presentations of a sucrose reward. Sucrose consumption prompted modest increases of in vivo BLA dopamine. Photometry traces were time locked to the first reward port entry after sucrose pump onset. B) Delivery of moderate 0.5mA footshocks evoked large BLA dopamine responses in the same rats. C) The footshock-evoked signal was larger than the BLA dopamine response to sucrose consumption when comparing AUC values. Data represent mean ± SEM. *p<0.05.

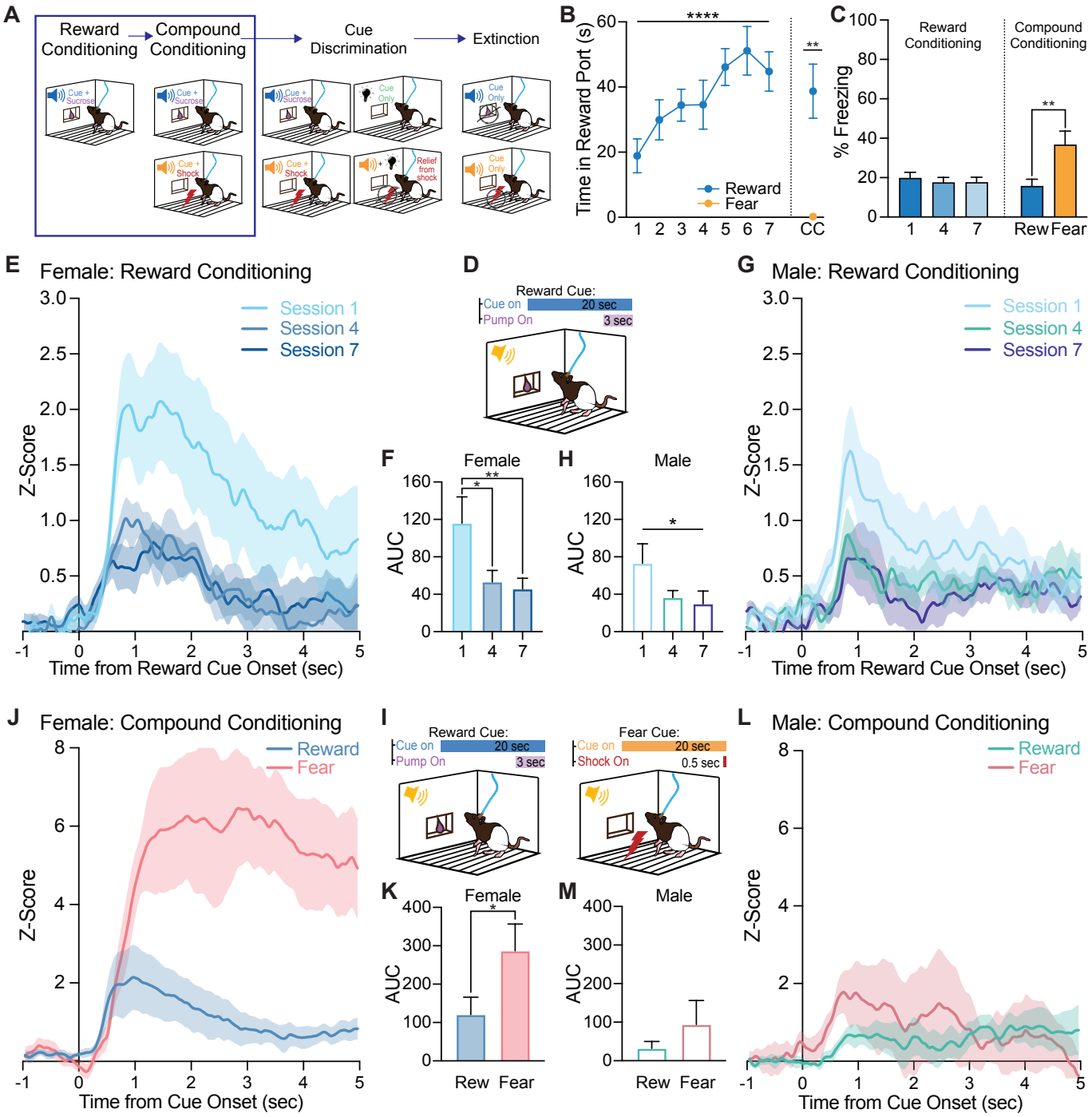

Fig 3 | Reward-cue evoked dopamine signals diminish with training but rebound in response to new cues preferentially in females

A) Schematic of the multi-phase Pavlovian cue discrimination paradigm (n=16; 9F, 7M). Behavior and photometry data for the first two phases: reward conditioning and compound (reward and fear) conditioning are shown. B) Throughout training, time spent in the reward port increased during reward cue presentations, while fear cue presentations did not prompt port entry behaviors. C) Cue-induced freezing was low for the reward cue during both reward and compound conditioning, but was higher for the fear cue in compound conditioning. D) During reward conditioning, a 20-s auditory cue was paired with a 3-s delivery of sucrose into the reward port. E) In females, reward cue evoked BLA dopamine responses were largest initially and decreased with training, F) as shown by AUC comparisons of the first 2 s after reward cue onset. G) In males, reward cue presentations also evoked larger BLA dopamine responses in early training that H) decreased with training. I) During compound conditioning (n= 9; 5F, 4M), trials containing a new 20 s auditory cue that predicted a footshock (0.5-s 0.5-mA) were intermingled with reward cue trials. J) Females exhibited large dopamine dynamics to the fear cue and moderate dopamine dynamics to the reward cue. K) The fear cue-evoked signal was greater than the reward cue when comparing AUC values. L) In males, the fear and reward cues produced similarly sized dopamine events, M) that did not show different AUC comparisons. Data represent mean ± SEM. *p<0.05, **p<0.01, ****p<0.0001.

ty cue that designates relief from shock (Sangha et al. 2013). We hypothesized that BLA dopamine transmission may be an important contributor to the disambiguation of differently valenced, salient events. Following fear plus reward compound conditioning rats were trained to distinguish between 4 different cues predicting various outcomes presented pseudorandomly during each cue discrimination behavioral session: the previously experi-

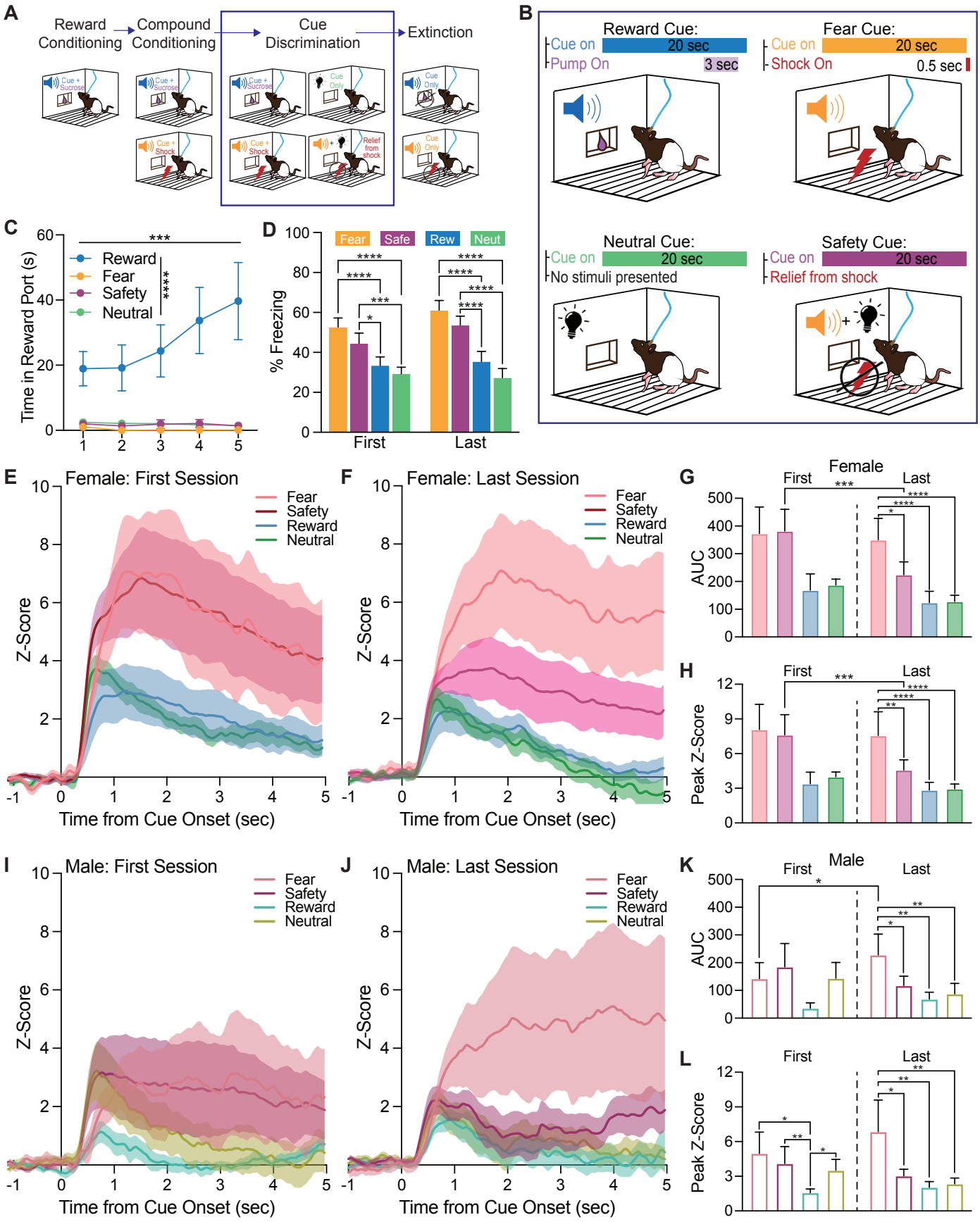

Fig 4 | Cue-evoked BLA dopamine dynamics scale with relative emotional saliency during discrimination learning

A) Schematic of the multi-phase Pavlovian cue discrimination paradigm the rats were trained on (n= 16; 9F, 7M). Behavior and photometry data from the valenced cue discrimination phase are shown. B) During the cue discrimination task, four cues were presented randomly throughout the two hour session. The previously learned reward and fear cues were intermingled with a neutral cue (20-s visual cue with no paired behavioral outcome) and a safety cue (20 s auditory fear and visual neutral cues presented together to signify relief from shock). C) Rats spent the highest amount of time in the reward port during the reward cue, and spent almost no time in the reward port during fear, safety, or neutral cue presentations. This discrimination grew across training days as rats increased their time in port during reward cue presentations. D) Cue-induced freezing remained high for the fear and safety cue throughout discrimination training, and was significantly higher than the reward and neutral cue freezing levels. E) In females, all four cue types elicited a positive peak on the first discrimination session, with the fear and safety cues prompting similar trace dynamics and the reward and neutral cues prompting similar trace dynamics. F) By the last discrimination session, the females had similar BLA dopamine release patterns, but the safety cue evoked much less dopamine compared to early training. G) AUC and H) peak measures of the BLA dopamine signals in females comparing the first and last discrimination session. I) In males, all cues evoked a positive BLA dopamine signal, with the reward cue qualitatively having the smallest trace, on the first discrimination session. J) By the last discrimination session, the fear cue produced the largest dopamine trace, in terms of peak and maintenance, while the safety, reward, and neutral cues produced modest and transient increases in BLA dopamine. K) AUC and L) peak measures of the BLA dopamine signals in females comparing the first and last discrimination session. Data represent mean ± SEM. *p<0.05, **p<0.01, ***p<0.001, ****p<0.0001.

enced (1) reward cue (paired with sucrose) and (2) fear cue (paired with a footshock), as well as a (3) neutral cue with no paired outcome and a (4) compound cue (fear+neutral cue played concurrently) to signal a relief or "safety" from shock (**Fig 4A,B**).

During this experimental phase, rats spent more time in the sucrose port during reward cue presentation periods than any other cue period (**Fig 4C**; F(3,45)=12.25, p<0.0001). They quickly discriminated cue types and this discrimination grew across sessions (**Fig 4C**; session x cue type interaction F(12,162)=3.333, p=0.0002). Further, cue-induced freezing was modulated by cue type (**Fig 4D**; F(3,45)=25.44, p<0.0001), with a graded response in freezing across fear, safety, reward, and neutral cues. Compared to the reward and neutral cues, the fear cue elicited more freezing behaviors in both the first (p<0.0001; p<0.0001) and last training session (p<0.0001; p<0.0001). The safety cue also evoked significantly more freezing than the reward cue (p=0.0205; p<0.0001) and the neutral cue presentations (p=0.0008; p<0.0001) on both the first and last cue discrimination days. There were no significant changes to reward or neutral cue freezing across training, which remained low. When comparing males and females, there were no significant differences in port entry behaviors to the reward, fear, or safety cues, however, males spent more time in the sucrose port during neutral cue presentations. There were no sex differences in cued freezing behaviors during the cue discrimination phase, however, by the final session, females were locomoting significantly more than males during the neutral and reward cue presentations (**Fig S2**).

Female BLA dopamine responds preferentially to fear and safety cues throughout discrimination learning

Prominent increases in BLA dopamine were seen in response to all cues in females during both the first (**Fig 4E**) and last (**Fig 4F**) discrimination training sessions. Dopamine signals were biased in magnitude according to cue type for AUC (**Fig 4G**; F(3,24)=9.587, p=0.0002) and peak value measures (**Fig 4H**, F(3,24)=6.420, p=0.0024), with the fear and safety cues evoking larger responses than the reward and neutral cues (**Fig 4E-H**). Early in discrimination training, the dopamine responses to the fear and safety cues were characterized by large peaks followed by a sustained elevation, while the reward and neutral cues prompted smaller peaks that more readily returned to baseline (**Fig 4E; Fig S3**). In contrast, by the last discrimination session, the reward and neutral cues maintained a similar evoked peak, but returned to baseline more quickly. By the last discrimination session, the fear cue elicited a similar high peak and sustained signal, but the safety cue signal diminished relative to session 1 (**Fig 4G,H**; AUC: p=0.0002; peak value: p=0.0003), reaching an intermediate level interposed between the fear cue trace and the reward and neutral cue traces (**Fig 4F**). On the last discrimination day, the fear cue signal had a larger peak value than all other cue types: safety cue (p=0.0019), reward cue (p<0.0001), and neutral cue (**Fig 4H**; p<0.0001). This pattern was consistent with the AUC values as well; fear cue presentations elicited larger and more sustained dopamine dynamics than the safety cue (p=0.0108), reward cue (p<0.0001), and neutral cue (**Fig 4G**; p<0.0001).

Male BLA dopamine responds preferentially to fear cues after discrimination learning

In males, all four cues elicited positive BLA dopamine transmission during both the first (**Fig 4I**) and last (**Fig 4J**) discrimination training sessions, with different cues prompting different dopamine levels as the sessions progressed (**Fig 4K**, AUC session x cue interaction, F(3,18)=3.829, p=0.0278; **Fig 4L**, main effect of cue type on evoked dopamine peak, F(3,18)=4.002, p=0.0240).

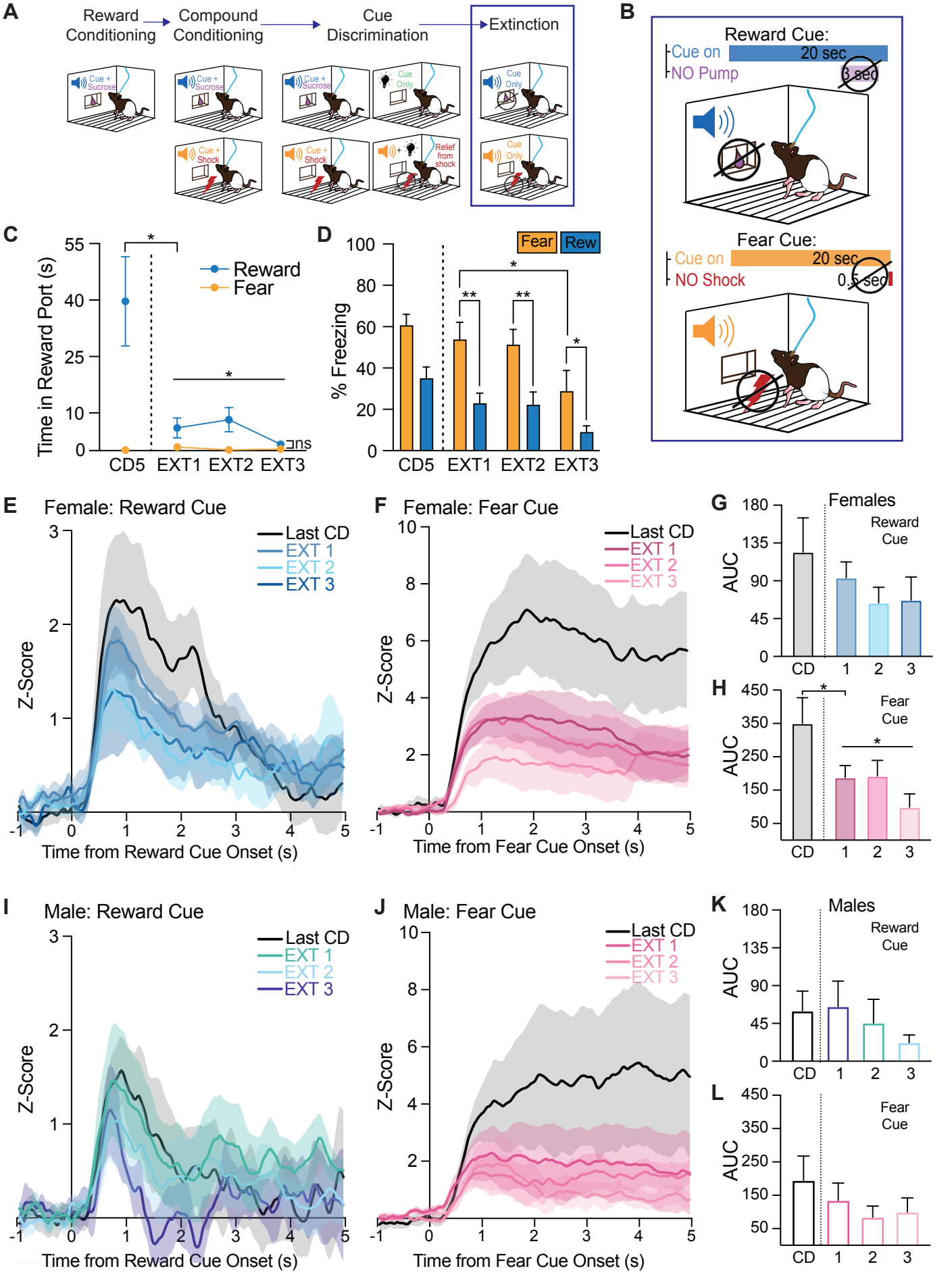
A
Reward Conditioning
Compound Conditioning
Cue Discrimination
Extinction
Cue + Sucrose
Cue Only
Cue + Shock
Relief from shock
B
Reward Cue:
Cue on
20 sec
NO Pump
3 sec
Fear Cue:
Cue on
20 sec
NO Shock
0.5 sec
C
Time in Reward Port (s)
Reward
Fear
ns
CD5 EXT1 EXT2 EXT3
D
% Freezing
Fear
Rew
CD5 EXT1 EXT2 EXT3
E
Female: Reward Cue
Last CD
EXT 1
EXT 2
EXT 3
Z-Score
Time from Reward Cue Onset (s)
F
Female: Fear Cue
Time from Fear Cue Onset (s)
G
Females
Reward Cue
AUC
CD 1 2 3
H
Fear Cue
I
Male: Reward Cue
J
Male: Fear Cue
K
Males
L

Fig 5 | Bias in extinction of reward versus fear cue-evoked BLA dopamine dynamics

A) Schematic of the multi-phase Pavlovian cue discrimination paradigm the rats were trained on (n=16; 9F, 7M). Behavior and photometry data from the extinction training phase are shown. B) The reward cue and fear cue were presented without their previously paired outcomes (sucrose or footshook). C) Compared to the last day of cue discrimination, port entry behaviors diminished during the reward cue when sucrose is omitted and remained absent during fear cue presentations. D) Cue induced freezing behavior decreased for the fear cue across extinction training, while freezing responses remained low for the reward cue. E) In females, the reward cue continued to elicit moderate BLA dopamine dynamics during extinction with similar levels to the final discrimination session, F) but the fear cue dopamine trace immediately decreased from the levels seen in the discrimination phase, and continued to temper down until the final extinction training day. G) Within extinction, AUC values also stayed constant for the reward cue, H) but decreased for the fear cue in females. This pattern was also seen when comparing AUC values from extinction day 1 to the final cue discrimination session. I) In males, cue-evoked BLA dopamine signals seen in the cue discrimination phase persisted during extinction training for both the reward cue J) and the fear cue. K) Corresponding AUC values did not significantly decrease for the reward cue L) nor the fear cue in males for either comparisons to the final discrimination session or within extinction training. Data represent mean ± SEM. *p<0.05, **p<0.01, ***p<0.001. CD=cue discrimination.

Notably, cue-evoked signals in males were uniformly smaller compared to the females, and the traces showed qualitatively different patterns. In the first discrimination session (**Fig 4I**), there were no differences between any of the AUC values (**Fig 4K**). The fear and safety evoked dopamine signals were not as sustained as seen in the females (**Fig 4E; Fig S3**) and the reward cue-evoked response was significantly smaller than the other cues (**Fig 4K**; fear: p=0.0460, safety: p=0.0044, neutral: p=0.0437). By the last discrimination session (**Fig 4J**), the fear cue response increased relative to session 1 (**Fig 4K**; p=0.0345), with the development of a sustained response compared to the more transient patterns seen with the other cue types. The fear cue elicited larger signals compared to all other cue types for AUC (**Fig 4K**; safety: p=0.0378, reward: p=0.0023, neutral: p=0.0071) and peak value (**Fig 4L**; safety: p=0.0272, reward: p=0.0048, neutral: p=0.0081). In contrast to the females, the safety, reward, and neutral cues evoked similar dopamine patterns in males.

Overall, in various conditioning contexts, we saw positive-going *in vivo* BLA dopamine signals during rewarding and aversive events and their predictive cues (**Fig 2-4**). Cue-evoked signals had clear qualitative distinction in the representation of different types of cues by the end of discrimination training in both females (**Fig 4E,F**) and males (**Fig 4I,J**). While there was a general bias toward the more fearful or ambiguous cues in both sexes, female dopamine responses were larger and more preferentially biased toward threat-related cues, in particular early in discrimination learning.

Bias in extinction of reward versus fear cue-evoked BLA dopamine dynamics

We next conducted extinction of cue discrimination (**Fig 5A**), wherein the reward and fear cues were presented without sucrose or footshock (**Fig 5B**). Conditioned behavioral responses extinguished quickly. When compared to the final day of cue discrimination, time spent in the reward port during reward cue presentations significantly decreased (**Fig 5C**; (t(11)=2.827, p=0.0165). Within extinction training, the time spent in the reward port during the reward cue presentations was generally greater than the fear cue presentations (**Fig 5C**; F(1,30)=4.878, p=0.0350), but this difference was gone by the third extinction session (**Fig 5C**; p=0.4323). Concurrently, cue-induced freezing behavior to the fear cue was higher than the reward cue (**Fig 5D**; F(1,30)=8.432, p=0.0069) throughout all of extinction training. This effect was blunted by the end of extinction as freezing to the fear cue was significantly lower on day 3 compared to day 1 (**Fig 5D**; p=0.0115). These behavioral changes, as well as cued locomotion levels, were similar in both females and males (**Fig S2**). However, the patterns and dynamics of the cue-evoked BLA dopamine established during discrimination training were well maintained throughout all three extinction sessions in both sexes for the reward cue (**Fig 5E,I**), but there were some changes in the encoding of the fear cue (**Fig 5F,J**). In females, dopamine responses did not decrease in response to the reward cue (**Fig 5E,G**; F(2,12)=2.696, p=0.1079) during extinction training or compared to the final discrimination session (t(8)=1.202, p=0.2638). However, the fear cue-evoked signal quickly decreased relative to cue discrimination (t(8)=2.752, p=0.0250) and continued to decrease as extinction training progressed (**Fig 5F,H**; F(2,12)=6.453, p=0.0125; day 3 vs day 1, p=0.0189 and day 2, p=0.0143). Meanwhile in males, the dopamine responses to both cues types were stable throughout extinction training (**Fig 5I-L**), with no significant changes in AUC for the reward cue (**Fig 5I,K**; t(8)=0.1881, p=0.8570; F(2,9)=1.544, p=0.2651) or fear cue (**Fig 5J,K**; t(8)=1.473, p=0.1911; F(2,9)=2.475, p=0.1392).

DISCUSSION

Here, we investigated how the BLA dopamine system is engaged as rats learned appetitive, aversive, and ambiguous associations. First, we show that VTA dopamine cell body and terminal stimulation robustly engages BLA dopamine signaling that is not intrinsically reinforcing. We then show that appetitive and aversive events, and

their predictive cues, evoke BLA dopamine signals in simple cue conditioning paradigms. Interestingly, cues evoked dopamine in a non-associative pattern, where signals were larger early and diminished across training. As we increased the complexity of the learning context, where cues signaling threat, reward, safety, and neutral associations were intermingled within a session, the level of cue-evoked BLA dopamine reported the relative perceived emotional salience: fear and safety cues elicited larger dopamine signals than either reward or neutral cues, a relative scaling that was apparent on the first discrimination session. These effects exhibited a sex bias, where females had larger cue-evoked dopamine dynamics than males, especially to threat-related stimuli, early in training. Together, our results show that BLA dopamine responds to salient cues, regardless of valence, and the magnitude and durability of these signals dynamically scales according to the emotional relevance of the stimulus. These unique patterns highlight a dopamine system that non-associatively encodes sensory state transitions in a way that is independent of value, to prime, rather than track, learning. Our data help expand conceptual frameworks of emotional learning and offer a number of new insights into amygdala and dopamine functions (Corder et al. 2019; Gründemann & Lüthi 2015; Gründemann et al. 2019; Kong et al. 2024, 2025; Ottenheimer et al. 2024; Sengupta et al. 2018; Tye & Janak 2007; Wojick et al. 2024; Zhang & Li 2018; Zhang et al. 2021).

Non-associative BLA dopamine signals prime learning

Our data suggest that instead of directly driving learning, VTA BLA dopamine inputs facilitate learning-related BLA mechanisms. We show that VTA dopamine neurons drive strong dopamine release in the BLA (Brinley-Reed & McDonald 1999; Lutas et al. 2019; Takahashi et al. 2010). While activation of VTA dopamine projections to the striatum is well documented to create associative learning and drive behavioral reinforcement (Kim et al. 2012; Steinberg et al. 2014; Witten et al. 2011; Wolff & Saunders 2024), we found that VTA-BLA dopamine signaling is not reinforcing to rats and BLA dopamine levels increase during both aversive and appetitive events, consistent with recent studies (Inglis & Moghaddam 1999; Sias et al. 2024). Together, this suggests that BLA dopamine does not directly signal the positive or negative aspects of stimuli, but is instead involved in the encoding, and subsequent disambiguation, of predictive sensory transitions. While there are other possible BLA dopamine sources, such as from the substantia nigra, periaqueductal gray, and dorsal raphe nucleus (Aksoy-Aksel et al. 2021; Mingote et al. 2015; Pinard et al. 2008; Poulin et al. 2018; Zhao et al. 2022), we hypothesize that input from VTA dopamine neurons is responsible for signaling the cued state changes we see in the BLA. This notion is supported by previous studies. Lesions of VTA dopamine neurons impair BLA cue attentional signals (Esber et al. 2012). VTA to BLA dopaminergic terminals are activated during learning (Lutas et al. 2019) and they are necessary for some aspects of reward and fear learning (Fadok et al. 2009; Sias et al. 2024). Further, there is heterogeneity of stimulus response profiles within populations of VTA dopamine neurons (Cai et al. 2020; Cohen et al. 2012; Elum et al. 2024; Jo et al. 2018; Morales & Margolis 2017; Park & Moghaddam 2017; Saunders et al. 2018; Schultz 2016), but a relatively anatomically uniform distribution of VTA to BLA projection neurons (Mingote et al. 2015; Tang et al. 2020). While it is unclear if they project to the BLA, a subset of VTA dopamine neurons are activated by both fear cues and non-predictive cues, suggesting the capacity to signal more general salience information (Jo et al. 2018). Our results suggest that dopamine inputs to the BLA play a role in learning about stimulus importance, possibly by modulating the activity of valence-sensitive ensembles. Meanwhile, the mediation of stimulus properties to represent valence is likely instead processed within the BLA via different populations of BLA neurons and/or through different efferent pathways to downstream regions (Namburi et al. 2015; Stuber et al. 2011). The BLA contains valence-sensitive clusters of neurons, where positive and negative conditioned stimuli are preferentially encoded (Beyeler et al. 2016, 2018; Gore et al. 2015; Gründemann et al. 2019; Namburi et al. 2015; O'Neill et al. 2018; Paton et al. 2006; Zhang & Li 2018; Zhang et al. 2021). These ensembles are anatomically interspersed but are largely separate and similarly sized populations. While there is clear evidence that some BLA neurons have inherent bias for representation of appetitive or aversive stimuli, the differential encoding of valence information among BLA neurons is dynamic with learning (Rogan et al. 2005; Sangha et al. 2013; Tye et al. 2008). Plasticity driving this discrimination is most likely supported by a complex array of circuit inputs and local communication within the amygdalar complex.

Notably, across experiments, BLA dopamine signal patterns did not fit with associative learning or prediction error frameworks - cue-evoked dopamine responses were generally strongest at the beginning of conditioning, before learning and subsequent behavioral discrimination. Further, these signals were engaged largely independent of valence and value, as novelty, threat, reward, and safety cues all evoked a positive excitation of dopamine release. This is in stark contrast to classic notions of the striatal dopamine system, where learning rate and prediction are reflected in incrementally accrued cue re-

sponses, and value is represented by negatively biased responses to aversive stimuli (Badrinarayan et al. 2012; Bornhoft et al. 2025; de Jong et al. 2019; Lammel et al. 2014; Lopez & Lerner 2025; McCutcheon et al. 2012; Oleson et al. 2012; Patriarchi et al. 2018; Roitman et al. 2008; van Elzelingen et al. 2022a). In comparison, the pattern of dopamine signals in the BLA imply they are not a readout of learning, but non-associatively prime the amygdala for learning. Our findings suggest that rather than signaling stimulus associability, BLA dopamine is involved in denoting sensory state transitions, where transmission is biased towards what is the most motivationally salient stimulus in the environment. Dopamine was released on a continuum with the most to fear cues, then safety, reward, and neutral cues - a scalar signal of inherent emotional salience. These data add novel insight into the growing understanding that dopamine neurons contribute heterogeneous information across projection sites (Bornhoft et al. 2025; Kutlu et al. 2021; Lammel et al. 2014; McCutcheon et al. 2012; van Elzelingen et al. 2022a,b). While additional experiments are needed to investigate this further, we hypothesize that rapid BLA dopamine fluctuations are critical for dynamic disambiguation between differently valenced stimulus contexts by priming amygdalar neurons for plasticity that allows for appropriate scaling of attention to the most important stimuli in the current environment.

We found that cue-evoked dopamine release attenuated over simple reward conditioning training, but when a valence contrast was introduced during compound conditioning, reward-cue signals rebounded. This pattern, which is again in contrast to classic associative dopamine patterns in the striatum, underscores the notion that BLA dopamine signals salient shifts in state and local stimulus context, rather than simply denoting either novelty or accrued learning. Consistent with this, past studies using microdialysis show that tonic dopamine levels in the BLA slowly increase while rats undergo discrimination learning (Hori et al. 1993), and pharmacologically boosting BLA dopamine enhances the early acquisition of a stimulus-reward association (Hitchcott et al. 1997). Further, in humans, dopamine is released in the amygdala during shifts from rest to working memory (Fried et al. 2001), suggesting that this system is engaged when memory of past associations are needed (Sias et al. 2021, 2024). In our data, we saw the most change over time in BLA dopamine in response to the safety cue, where signals were initially larger and comparable to the fear cue, but decreased in both sexes as discrimination learning progressed. These patterns support the notion that BLA dopamine is not purely biased towards negatively-valenced events but, more broadly, is invigorated and then reinvigorated when novel cues in the environment are introduced, as a possible way to drive encoding of the relative importance of different elements of the current environment. Collectively, our results and other recent studies (Sias et al. 2024), support a framework where BLA dopamine contributes preferentially to flexible model-based learning, rather than reward prediction error, incentive motivation, or reinforcement.

BLA dopamine tracks emotional salience

We found that some cues evoked not only greater peak BLA dopamine, but also sustained increases throughout the cue period. Fear cue-evoked signals were larger and broader across each presentation, while reward and neutral cue signals were smaller and featured a quicker return to baseline. Interestingly, the safety cue evoked an intermediate response that was sustained but smaller than the fear cue signal. This scaling of sustained dopamine matches the perceived emotional vigilance state. These patterns are wholly distinct from cue-evoked dopamine signals in striatum, which are typically composed of rapid phasic fluctuations (Badrinarayan et al. 2012; Bornhoft et al. 2025; de Jong et al. 2019; Lammel et al. 2014; Lopez & Lerner 2025; McCutcheon et al. 2012; Oleson et al. 2012; Patriarchi et al. 2018; Roitman et al. 2008; van Elzelingen et al. 2022a). Mechanistically, sustained BLA dopamine patterns may be supported by the relatively low levels of the dopamine transporter (DAT) and slower dopamine clearance rates within the amygdala, compared to the striatum (Holleran et al. 2020; Revay et al. 1996). Further, dopamine neurons projecting to the BLA are known to exhibit unique physiological characteristics (Ford et al. 2006; Margolis et al. 2006), preferentially targeting BLA projection neurons containing the D1-type dopamine receptors (D1DR) (Aksoy-Aksel et al. 2021; Kröner et al. 2005; Muller et al. 2009; Scibilia et al. 1992; Takahashi et al. 2010). Optogenetic activation of dopamine release increases cyclic AMP activity in BLA D1DR neurons and enhances their response to sensory inputs (Lutas et al. 2022), while pharmacological activation of BLA D1DR signaling facilitates contextual fear learning (Heath et al. 2015), freezing behavior (Guarraci et al. 1999), reward seeking and learning (Tye et al. 2010), as well as safety cue-induced fear suppression (Ng et al. 2018). Our results suggest that moment-to-moment dopamine signals may fine tune these D1-containing BLA projection neurons, priming them to the attentional needs of incoming cues, to influence the output of conditioned behaviors in distal regions. Further, variability in sustained levels of dopamine during discrimination of different cues likely supports stimulus context encoding via such dopamine-induced plasticity.

In our hands, female rats consistently exhibited larger dopamine responses compared to males during cue presentations, in particular for threat and safety cues. This adds important context to previous studies where sex differences were not isolated (Lutas et al. 2019; Morishita et al. 2024; Sias et al. 2024). Our data suggest that the female BLA dopamine system is more sensitive to novel threats or more highly engaged with early discrimination learning compared to males. BLA dopamine may come online more strongly initially for females in discrimination training as they use this signal to gain and modulate information about valence and motivational saliency, while this signal takes more time and learning to evolve in males undergoing discrimination learning. This interpretation is supported by the dopamine response to the initially threatening safety cue in females, which then gets turned down as learning occurred. In contrast, in males the dopamine response to the fear cue started moderate, but grew as the threat was firmly established. In our studies, the viral expression and optic fiber placements were similar in the males and females, and there were no consistent sex differences in conditioned behaviors or movement. These results are interesting in light of previous data showing a wide range of sex differences in behavioral threat and safety responses (Chowdhury et al. 2019; Greiner et al. 2019; Gruene et al. 2015; Orsini et al. 2016; Yokota et al. 2017), suggesting complex and distinct fear response strategies between female and male rodents. While we found no obvious connection between cue-evoked dopamine and behavior in males and females, this signal may be used to support behavioral vigilance and decision making in sex-biased ways within the amygdala (Wheeler et al. 2024).

Here we showed BLA dopamine release tracked both the cue and the paired outcome in many different kinds of learning: reward, fear, compound, discrimination, and extinction. Taking the working hypothesis that the BLA processes sensory stimuli on both the proximal and environmental levels and then transforms that information to emotional and behavioral outputs, we demonstrated that BLA dopamine signals were non-associatively involved in valence discrimination via a transmission bias that reported the initial relative emotional saliency, where fear and ambiguous cues evoked higher levels of dopamine than reward and innocuous cues. We suggest that dopamine transmission primes amygdalar neurons for valence encoding and learning-related plasticity. Our results support a framework where the BLA dopamine system, in contrast to classic striatal dopamine frameworks, serves as a general, state-guided saliency signal to support emotional learning via non-associative mechanisms. This signal is dynamically engaged in a learning context where relative stimulus importance must be rapidly disambiguated.

Funding and Acknowledgements
The authors have no biomedical financial interest or potential conflicts of interest. This work was supported by NIH grants F31 DA060004 (MAB), P30 DA048742 (MJT), and R00 DA042895, R01 MH129370, R01 MH129320, and R01 DA057292 (BTS). The authors thank all members of the Thomas and Saunders labs for technical support and feedback.

METHODS

Subjects

Male and female Long Evans rats (n=20; 10F, 10M) were used. All rats weighed 250-500g at the time of surgery and were 4-9 months old at the time of experimentation. Experimental procedures were approved by the Institutional Animal Care and Use Committee at the University of Minnesota and were carried out in accordance with the guidelines on animal care and use of the National Institutes of Health of the United States.

Surgical Procedures

Rats were anesthetized with 5% isoflurane and placed in a stereotaxic frame, after which anesthesia was maintained at 1-3%. Saline, carprofen anesthetic (5 mg/kg), and cefazolin antibiotic (70 mg/kg) were administered subcutaneously prior to start of surgery. The top of the skull was exposed and holes were made for viral infusion needles, optic fiber implants, and 4 skull screws. A total of 0.5 µL of a virus coding for the dopamine biosensor dLight 1.3b (AAV5-hSyn-dLight1.3b, University of Minnesota Viral Vector and Cloning Core) was infused unilaterally into the BLA (2.7 AP, +/- 4.9 ML, -8.2 DV). In a separate cohort of rats, a total of 1.2 µL of virus (pAAV5-Syn-FLEX-Chrimson-tdTomato, Addgene) was infused unilaterally into the VTA (−5.6 AP, +/− 0.7 ML, −8.0 DV), while dLight1.3b injections were targeted to the ipsilateral BLA. Each virus was delivered at 0.1µL/min. Immediately after injection, the needle was raised 100 µm and then left in place for an additional 10 min to allow for diffusion. Optical fibers (9mm length, 400µm diameter, Doric Lenses) for photometry recordings were chronically implanted into the BLA (2.7 AP, +/- 4.9 ML, -7.9 DV) in the same hemisphere as the viral infusion. For optogenetic stimulation, optical fibers (10mm length, 300µm diameter, Thorlabs) were implanted above the VTA (−5.6 AP, +/− 0.7 ML, −7.9 DV) in the same hemisphere of viral injections. All coordinates are in mm relative to bregma and skull surface. Implants were secured to the skull with dental acrylic (Lang Dental) applied around the skull screws and the base of the ferrules containing the optic fibers. At the end of all surgeries, topical anesthetic and antibiotic ointment

were applied to the surgical site, rats were placed on a heating pad and monitored until they were ambulatory. After surgery rats were individually housed with ad libitum access to food and water on a 0800 to 2000 light/dark cycle (lights on at 0800), given carprofen (5 mg/kg) and cefazolin (70 mg/kg) for the first 3 days following surgery and weighed and monitored for 6 days. Photometry recordings began at least 3 weeks after surgery. Optogenetic manipulations started at least 6 weeks after surgery.

Fiber Photometry Recordings

Behavioral testing days were paired with fiber photometry recording to measure dopamine signals (n=19; 10F, 9M) in the BLA. The fiber photometry system was outfitted with optical components from Doric Lenses (Québec, Canada). This included fluorescence mini-cubes to transmit concurrent light streams from LEDs, 465nm and 405/415nm, that were sinusoidally modulated at 211Hz and 330Hz, respectively. The 465nm channel stimulated fluorescence from the dopamine-dependent dLight, while the 405/415nm served as an isosbestic reference that excites dLight in a dopamine-independent manner. Demodulating the brightness produced by both channels allows for reliable correction of movement or photobleaching artifacts. Before each photometry recording both LED currents were set to ~50µW. Fluorescence was transmitted from the fiber tip over the BLA back to the mini-cube via an optic cable, where it was passed through a GFP emission filter, amplified and directed into a high sensitivity photoreceiver (Newport, Model 2151) for signal processing. Meanwhile, the session was controlled and data was acquired via Synapse software running on a Tucker-Davis Technologies (TDT, Alachua, FL) real-time processor (RZ5P), as reported in previous studies (Bornhoft et al. 2025; Engel et al. 2024). Synapse software on the RZ5P processor calibrated the output of each LED channel and simultaneously recorded photometry signals, which were being sampled from the photodetector at 6.1 kHz. To align the real-time neural signals to behavioral (e.g., port entries) and environmental (e.g., cue presentations) occurrences, TTL signals from the operant chambers (Med Associates) were sent to the RZ5P processor and timestamped for post-hoc analysis of the photometry data. Video recordings were also taken and integrated with the photometry and behavior data via the Synapse software.

Optogenetic Stimulation and Behavior

Optogenetic stimulation: These studies used 589-nm lasers (OptoEngine and Dragon Lasers). Light output included individual 5ms light pulses for either 5Hz or 20Hz stimulation frequency. Light intensity was adjusted to be approximately 2 mW/mm2 at the tip of the intracranial fiber during individual pulses (~10-mW constant power). The optic tethers connected to the rats were sheathed in a lightweight armored jacket to block visible light transmission and reinforce the cable to prevent breakage. Laser pulses were initiated from Med-PC TTL pulses and patterned via Synapse software that also controlled photometry and video data acquisition. Fiber photometry recordings were concurrently collected on every optogenetic training day.

Fiber Photometry and Optogenetic Behavior: To understand how VTA TH-neuron activity influences dopamine dynamics in the BLA, *in vivo* optogenetics was paired with fiber photometry in TH-Cre rats (n= 3; 1F, 2M). Rats were first acclimated to the behavioral chambers (Med Associates) and optic cable tethering in a ~30-min habituation session. During VTA TH-cell body stimulation, an optic tether was attached over the VTA implant to deliver optogenetic stimulation while another was attached to the BLA implant for dLight fiber photometry data collections. In separate sessions, rats were tethered to the optic cable and presented with 10 laser stimulations on a 120-s fixed time schedule. The stimulation parameters were (1) 5Hz stimulation for 2 s, (2) 20Hz stimulation for 2 s, (3) 5Hz stimulation for 5 s, and (4) 20Hz stimulation for 5 s. These stimulation presentations were un-cued and not paired with any external stimulus. The same stimulation parameters and sessions were repeated for VTA TH-neuron terminal stimulation over the BLA. Here, the optic tether connected to the BLA implant concurrently delivered the laser stimulation, while collecting dLight fiber photometry fluorescence signals.

Intracranial self-stimulation (ICSS): We expressed Chrimson in VTA dopamine neurons in TH-Cre rats (n= 4; 1F, 3M) and inserted an optic fiber in the BLA. Rats were placed in the testing chamber (Med Associates) and connected to an optic cable tether to receive optogenetic stimulation to target VTA dopamine terminals in the BLA. Two nose poke ports were positioned on one side of the chamber. Nose pokes in the active port resulted in a 2-s laser train (20Hz, 5-ms pulses, fixed-ratio 1 schedule) that coincided with the delivery of a tri-color light illumination cue. Laser stimulation parameters were chosen to align with the results from the fiber photometry studies above where 2-s, 20Hz VTA-BLA dopamine terminal stimulation prompted reliable dopamine dynamics in the BLA.

Pavlovian Cue Discrimination Behavioral Assay

All Pavlovian behavior training began at least 3-4 weeks after surgery. Med Associates chambers were outfitted with a syringe pump to deliver liquid sucrose reward, a magazine port equipped with an infrared beam to

sense port entries, floor bars for the delivery of electrical shocks, speakers for the delivery of tone (high: 4500 Hz, low: 2900 Hz), and house lights for illumination. Cameras were positioned above each chamber to record movement throughout each session for post-hoc behavioral analysis. Port entry instances and durations were recorded by Med Associates software throughout the sessions. Chambers were cleaned with 70% ethanol and bedding was replaced after each session.

This Pavlovian cue discrimination task (n= 16; 9F, 7M) was adapted from previous studies (Sangha et al. 2013). Habituation: Training began with acclimation to the behavioral chambers and optic cable tethering in two ~30 minute habituation sessions. During these sessions, rats were tethered to the fiber photometry cable and allowed to freely move and explore around the chamber.

Reward Conditioning: For the 7 following sessions, rats were presented with 25 auditory cue presentations lasting 20 s each on 110 s variable time (VT) schedule, (range: 90-130 s). The auditory cue was either a pulsing low tone (repeating cycle of 0.2 s on and 0.2 s off) or a continuous high tone counterbalanced across rats. Each reward cue presentation was paired with a liquid reward (10% sucrose) delivered pseudorandomly between 10 s and 20 s after the reward cue onset. Each session lasted ~55 min.

Cue Habituation: To acclimate the rats to the remaining cues, during an 8th reward conditioning session (25 auditory reward cue+sucrose presentations), the rats were pseudorandomly presented with noncontingent cues (5 house lights illuminations, 5 auditory (counterbalanced high or low) tones) lasting 20 s each. These cue presentations were not associated with any outcome. This session lasted ~75 min.

Compound Conditioning: The next training session introduced the fear cue - 5 presentations of a 20-s auditory cue paired with a mild footshock (0.4 mA) delivered from 19.5-20 s. The fear cue presentations were pseudorandomly delivered intermixed with 25 reward cue presentations. This session lasted ~65 min.
Cue Discrimination: After initial learning, the rats underwent the cue discrimination phase of the paradigm. Here, the rats had to distinguish between 4 different cues predicting various outcomes: the previously introduced (1) reward cue (paired with sucrose) and (2) fear cue (paired with a footshock), as well as a (3) neutral cue with no paired outcome and a (4) compound cue (fear+neutral cue played concurrently) to signal a relief from shock. The high and low tones, as well as pulsatile versus continuous tones, were counterbalanced across rats for the reward and fear cues. House light illumination was always used for the neutral cue. The compound cue signaling relief from shock was always the fear cue (counterbalanced auditory cue) played concurrently with the neutral cue (visual cue) for 20 s. There were 45 total cue presentations in each training session (15 reward cues, 5 fear cues, 10 neutral cues, and 15 compound cues). Each cue lasted 20 s and was delivered in pseudorandom orders on a 110 s average VT schedule (range 90-130 s). Each animal had 4-6 cue discrimination sessions, each lasting ~100 min.

Extinction: Behavioral testing concluded with 2-3 extinction sessions. Here, only the reward and fear cues were presented (20 presentations each; pseudorandom order) and both the reward and shock deliveries were omitted. These sessions lasted ~85 min each.

DeepLabCut-based pose tracking

Markerless tracking of animal body parts was conducted using the DeepLabCut Toolbox (DLC version 2.2.3) (Mathis et al. 2018) and analysis of movement features based on these tracked coordinates was conducted in Matlab R2024b (Mathworks). All DLC analysis was conducted on either an Alienware Aurora R13 Gaming desktop running Windows 11 with an Intel Core i9-12900F CPU, 2400 Mhz, 128 GB RAM, and an NVIDIA GeForce RTX 3090 32GB GPU or a Dell G7-7590 laptop running Windows 10 with an Intel Core i7-9750H CPU, 2.60Ghz, 16GB RAM, and an NVIDIA GeForce RTX 2080 Max-Q 8GB GPU. DeepLabCut was installed in an Anaconda environment with Python 3.8.15, CUDA 12.0 and Tensorflow 2.10.0. Videos (944 × 480 resolution) were recorded with a sampling frequency of 10-20 frames per second using TDT Synapse software with overhead cameras (Vanxse CCTV 960H 1000TVL HD Mini Spy Security Camera 2.8-12 mm Varifocal Lens Indoor Surveillance Camera).

DeepLabCut Model: Videos from this experiment were analyzed through a refined DLC network as described previously (Bornhoft et al. 2025; Engel et al. 2024). To create the network, the body parts labeled included the nose, eyes, ears, fiber optic implant, shoulders, tail base, and an additional three points along the spine. Features of the environment were also labeled, including the 4 corners of the apparatus floor and the two magazine ports. Briefly, 2090 frames from 35 videos (32 different animals, 3 experiments) were labeled and 807 outlier frames were relabelled to refine the network for the current study. Labeled frames were split into a training set (95% of frames) and a test set (5% of frames). A ResNet-50 based neural network was used for 1,030,000 training iterations. After final refinement, we used a p-cutoff of 0.85 resulting in training set error

of 2.99 pixels and test set error of 3.68 pixels. This model was then used to analyze videos from the rats (n=16; 9F, 7M) who underwent the cue discrimination behavioral assay for all training sessions.

Data Analysis

Behavioral Analysis:

Port entries, locomotion bouts, and freezing bouts were the primary behavioral output measures. Port entry frequency and duration was analyzed from MedPC software outputs and the generated TTL signals from Synapse.

Video Scoring: Freezing data was first analyzed with hand-scoring of recorded videos from the cue discrimination training sessions. For each animal, freezing duration for each cue presentation was calculated during at least the first and last cue discrimination training session. The experimenter was blinded for both rat and session information. Cue-evoked freezing was timed for each cue three times and the average was calculated.

DeepLabCut Analysis: Freezing bouts and locomotion bouts were also calculated from positional information tracked using DLC. Bodypart coordinates and confidence values for each video frame were determined by the DLC network and were analyzed with Matlab. Broadly, any frames with body part coordinates where confidence values were below 0.7 were excluded from further data processing. The average coordinates of fixed features of the operant chamber were used for analysis. A pixel-to-cm ratio was calculated for each processed video in order to transform pixel distances into physical chamber dimensions for subsequent distance traveled and speed analyses. The pixel distance of all 4 perimeter sides and both diagonal cross-sections were determined, divided by the actual distance in cm, then that quotient value is averaged to give the pixel-to-cm conversion for each video. Movement speed was calculated from the coordinates of the mid-back, for each video frame, the formula [distance moved (pix per cm) * framerate] was used to provide movement speed in cm/s. For analyzing data across recordings with different sampling rates, missing data points for the lower sampling rate sessions were filled in using linear interpolation with the interpol1 function (MATLAB). Interpolated data points were not used to calculate peak or mean speeds for analysis.

Freezing and locomotion detection was uniquely computed for each animal using a movement threshold determined by animal body size (distance between shoulder and lower back) and the predetermined optimal threshold for movement detection based on our operant chamber configuration (Bornhoft et al. 2025; Engel et al. 2024). This threshold value was used to detect fine movement in the face and head; for movement detection in the body, the limit was multiplied by 2 to account for larger body parts. Freezing bouts were defined as all visible body parts being below their corresponding movement threshold for any single video frame, while the transitions in and out of a movement bout were demarcated by a sliding window when the speed of 2 or more body parts exceeded the detection threshold for 0.2 s. For all bouts, video frames where less than 2 body parts were visible were excluded. For freezing, bouts lasting under 1 s were excluded from bout analysis. Locomotion was detected using the speed of the implant and 4 locations on the spine. Locomotion bouts were determined if all visible body parts were above their corresponding movement threshold for any single video frame, while the transitions in and out of a movement bout were demarcated by a sliding window when the speed of 2 or more body parts exceeded the detection threshold for 0.3 s. For locomotion, bouts lasting less than 0.5s were excluded from bout analysis.

Fiber Photometry Analysis:

Photometry data were analyzed using a custom MATLAB pipeline and GraphPad Prism. First, the photometry signals (both 405nm/415nm isosbestic and 465nm) were low pass filtered and downsampled to 40Hz. The isosbestic signal was then aligned to the 465-nm signal by applying a least-squares linear fit and this fitted isosbestic signal was used to normalize the 465-nm signal, where $\Delta F/F$ = (465 nm signal – fitted 415-nm signal)/(fitted 415-nm signal). Timestamps for each video recording (recorded at 10-20 FPS) were recorded in the Synapse photometry data file. Cue presentations, port entries, sucrose pumps, and footshocks were assigned a TTL signal from Med-PC that was used to timestamp the photometry data file in the Synapse software. The normalized $\Delta F/F$ signals were extracted 5 s before and 25 s following each cue presentation and Z-scored to the 5 s pre-cue period for each trial to minimize the effects of drift in the signal across experiment duration. Normalized signals for reward consumption were extracted in the window from 2 s preceding to 4 s following each port entry and Z-scored to the 2 s pre-port entry. Port entry occurrences were binned into rewarded and unrewarded port entries. The first port entry after reward delivery with a duration of >0.5 s was designated a rewarded port entry. Normalized signals for shock responses were extracted in the window from 2 s preceding to 4 s following each shock delivery and Z-scored to the 2 s pre-shock delivery. Cue responses were detected in the average waveform for each animal in the 5 s window beginning at cue onset, while reward and shock responses used a 2 s window beginning at event onset. The maximum and minimum responses in each window were detected, and latency to the maximum

or minimum was calculated relative to the start of the detection window. Area under the curve (AUC) values were calculated from the Z-scored traces by numerical integration via the trapezoidal method using the trapz function (Matlab).

Statistics:
Behavior and photometry signal data were analyzed with a combination of ANOVA models (one-way, two-way, and mixed effects) and t-tests. Post-hoc comparisons and planned t-tests were used to clarify main effects and interactions. Graphs represent average values of sites/subjects, not individual trials. The data are expressed as the mean ± s.e.m. For all tests, the statistical significance was set at $p<0.05$.

Histology
Rats were deeply anesthetized via i.p. injections of Fatal-Plus (2 ml/kg; Paterson Veterinary) and were transcardially perfused with cold phosphate buffered saline (PBS) and subsequent 4% paraformaldehyde (PFA). Brains were extracted and continued to be fixed in 4% PFA overnight (~24 hrs) then were transferred to a cryoprotectant solution of 30% sucrose in PBS for at least 48 hrs. The tissue was cut into 50-µm sections on a freezing microtome (Leica Biosystems) and brain sections containing the BLA were mounted on microscope slides and coverslipped with Vectashield containing DAPI counterstain to validate viral expression and proper optic fiber placements. Images of the microscope slides were taken on a fluorescent microscope (Keyence BZ-X710) with a 4x and a 10x air immersion objective. Virus spreads and fiber positions were compared to the Rat Brain Atlas (Paxinos and Watson, 2007) and plotted with Adobe Illustrator.

Immunohistochemistry:
To visualize dopamine projections in the amygdala, we performed immunohistochemistry for tyrosine hydroxylase. Brain sections were washed in PBS and incubated with bovine serum albumin (BSA) and Triton X-100 (each 0.2%) for 20 min. 10% normal donkey serum (NDS) was added for a 30-min incubation, before primary antibody incubation (rabbit anti-TH, 1:500, Invitrogen) overnight at 4°C in PBS with BSA and Triton X-100 (each 0.2%). Sections were then washed and incubated with 2% NDS in PBS for 10 minutes and secondary antibodies were added (1:200 594 donkey anti-rabbit) for 2 hours at room temperature. Sections were washed 2 times in PBS and mounted with Vectashield containing DAPI.

REFERENCES

Aksoy-Aksel A, Gall A, Seewald A, Ferraguti F, Ehrlich I. 2021. Midbrain dopaminergic inputs gate amygdala intercalated cell clusters by distinct and cooperative mechanisms in male mice. eLife. 10:

Badrinarayan A, Wescott SA, Vander Weele CM, Saunders BT, Couturier BE, et al. 2012. Aversive stimuli differentially modulate real-time dopamine transmission dynamics within the nucleus accumbens core and shell. J. Neurosci. 32(45):15779–90

Beyeler A, Chang C-J, Silvestre M, Lévêque C, Namburi P, et al. 2018. Organization of Valence-Encoding and Projection-Defined Neurons in the Basolateral Amygdala. Cell Rep. 22(4):905–18

Beyeler A, Namburi P, Glober GF, Simonnet C, Calhoon GG, et al. 2016. Divergent Routing of Positive and Negative Information from the Amygdala during Memory Retrieval. Neuron. 90(2):348–61

Bornhoft KN, Prohofsky J, O'Neal TJ, Wolff AR, Saunders BT. 2025. Striatal dopamine represents valence on dynamic regional scales. J. Neurosci.

Brinley-Reed M, McDonald AJ. 1999. Evidence that dopaminergic axons provide a dense innervation of specific neuronal subpopulations in the rat basolateral amygdala. Brain Res. 850(1–2):127–35

Cador M, Robbins TW, Everitt BJ. 1989. Involvement of the amygdala in stimulus-reward associations: interaction with the ventral striatum. Neuroscience. 30(1):77–86

Cai LX, Pizano K, Gundersen GW, Hayes CL, Fleming WT, et al. 2020. Distinct signals in medial and lateral VTA dopamine neurons modulate fear extinction at different times. eLife. 9:

Chowdhury TG, Wallin-Miller KG, Rear AA, Park J, Diaz V, et al. 2019. Sex differences in reward- and punishment-guided actions. Cogn. Affect. Behav. Neurosci. 19(6):1404–17

Cohen JY, Haesler S, Vong L, Lowell BB, Uchida N. 2012. Neuron-type-specific signals for reward and punishment in the ventral tegmental area. Nature. 482(7383):85–88

Corder G, Ahanonu B, Grewe BF, Wang D, Schnitzer MJ, Scherrer G. 2019. An amygdalar neural ensemble that encodes the unpleasantness of pain. Science. 363(6424):276–81

Correia SS, Goosens KA. 2016. Input-specific contributions to valence processing in the amygdala. Learn. Mem. 23(10):534–43

de Jong JW, Afjei SA, Pollak Dorocic I, Peck JR, Liu C, et al. 2019. A neural circuit mechanism for encoding aversive stimuli in the mesolimbic dopamine system. Neuron. 101(1):133-151.e7

Duvarci S, Pare D. 2014. Amygdala microcircuits controlling learned fear. Neuron. 82(5):966–80

Elum JE, Szelenyi ER, Juarez B, Murry AD, Loginov G, et al. 2024. Distinct dynamics and intrinsic properties in ventral tegmental area populations mediate reward association and motivation. Cell Rep. 43(9):114668

Engel L, Wolff AR, Blake M, Collins VL, Sinha S, Saunders BT. 2024. Dopamine neurons drive spatiotemporally heterogeneous striatal dopamine signals during learning. Curr. Biol. 34(14):3086-3101.e4

Esber GR, Roesch MR, Bali S, Trageser J, Bissonette GB, et al. 2012. Attention-related Pearce-Kaye-Hall signals in basolateral amygdala require the midbrain dopaminergic system. Biol. Psychiatry. 72(12):1012–19

Everitt BJ, Morris KA, O'Brien A, Robbins TW. 1991. The basolateral amygdala-ventral striatal system and conditioned place preference: further evidence of limbic-striatal interactions underlying reward-related processes. Neuroscience. 42(1):1–18

Fadok JP, Dickerson TMK, Palmiter RD. 2009. Dopamine is necessary for cue-dependent fear conditioning. J. Neurosci. 29(36):11089–97

Fields HL, Hjelmstad GO, Margolis EB, Nicola SM. 2007. Ventral tegmental area neurons in learned appetitive behavior and positive reinforcement. Annu. Rev. Neurosci. 30:289–316

Ford CP, Mark GP, Williams JT. 2006. Properties and opioid inhibition of mesolimbic dopamine neurons vary according to target location. J. Neurosci. 26(10):2788–97

Fried I, Wilson CL, Morrow JW, Cameron KA, Behnke ED, et al. 2001. Increased dopamine release in the human amygdala during performance of cognitive tasks. Nat. Neurosci. 4(2):201–6

Gore F, Schwartz EC, Brangers BC, Aladi S, Stujenske JM, et al. 2015. Neural representations of unconditioned stimuli in basolateral amygdala mediate innate and learned responses. Cell. 162(1):134–45

Greiner EM, Müller I, Norris MR, Ng KH, Sangha S. 2019. Sex differences in fear regulation and reward-seeking behaviors in a fear-safety-reward discrimination task. Behav. Brain Res. 368:111903

Gruene TM, Flick K, Stefano A, Shea SD, Shansky RM. 2015. Sexually divergent expression of active and passive conditioned fear responses in rats. eLife. 4:

Gründemann J, Bitterman Y, Lu T, Krabbe S, Grewe BF, et al. 2019. Amygdala ensembles encode behavioral states. Science. 364(6437):

Gründemann J, Lüthi A. 2015. Ensemble coding in amygdala circuits for associative learning. Curr. Opin. Neurobiol. 35:200–206

Guarraci FA, Frohardt RJ, Kapp BS. 1999. Amygdaloid D1 dopamine receptor involvement in Pavlovian fear conditioning. Brain Res. 827(1–2):28–40

Heath FC, Jurkus R, Bast T, Pezze MA, Lee JLC, et al. 2015. Dopamine D1-like receptor signalling in the hippocampus and amygdala modulates the acquisition of contextual fear conditioning. Psychopharmacology (Berl). 232(14):2619–29

Hitchcott PK, Harmer CJ, Phillips GD. 1997. Enhanced acquisition of discriminative approach following intra-amygdala d-amphetamine. Psychopharmacology (Berl). 132(3):237–46

Holleran KM, Rose JH, Fordahl SC, Benton KC, Rohr KE, et al. 2020. Organic cation transporter 3 and the dopamine transporter differentially regulate catecholamine uptake in the basolateral amygdala and nucleus accumbens. Eur. J. Neurosci. 52(11):4546–62

Hori K, Tanaka J, Nomura M. 1993. Effects of discrimination learning on the rat amygdala dopamine release: a microdialysis study. Brain Res. 621(2):296–300

Inglis FM, Moghaddam B. 1999. Dopaminergic innervation of the amygdala is highly responsive to stress. J. Neurochem. 72(3):1088–94

Janak PH, Tye KM. 2015. From circuits to behaviour in the amygdala. Nature. 517(7534):284–92

Jo YS, Heymann G, Zweifel LS. 2018. Dopamine neurons reflect the uncertainty in fear generalization. Neuron. 100(4):916-925.e3

Khalil V, Faress I, Mermet-Joret N, Kerwin P, Yonehara K, Nabavi S. 2023. Subcortico-amygdala pathway processes innate and learned threats. eLife. 12:

Kim KM, Baratta MV, Yang A, Lee D, Boyden ES, Fiorillo CD. 2012. Optogenetic mimicry of the transient activation of dopamine neurons by natural reward is sufficient for operant reinforcement. PLoS ONE. 7(4):e33612

Kong M-S, Ancell E, Witten DM, Zweifel LS. 2025. Valence and salience encoding in the central amygdala. eLife. 13:

Kong M-S, Jo YS, Sethi E, Pyeon GH, Zweifel LS. 2024. A dopamine-dependent mechanism for Reward-induced modification of Fear memories. BioRxiv

Kröner S, Rosenkranz JA, Grace AA, Barrionuevo G. 2005. Dopamine modulates excitability of basolateral amygdala neurons in vitro. J. Neurophysiol. 93(3):1598–1610

Kutlu MG, Zachry JE, Melugin PR, Cajigas SA, Chevee MF, et al. 2021. Dopamine release in the nucleus accumbens core signals perceived saliency. Curr. Biol. 31(21):4748-4761.e8

Lammel S, Lim BK, Malenka RC. 2014. Reward and aversion in a heterogeneous midbrain dopamine system. Neuropharmacology. 76 Pt B(0 0):351–59

Leppla CA, Keyes LR, Glober G, Matthews GA, Batra K, et al. 2023. Thalamus sends information about arousal but not valence to the amygdala. Psychopharmacology (Berl). 240(3):477–99

Li Z, Qu Y, Wu Q-L, Tang L, Dong Y, Xu X-F. 2025. Input-output organization of the mouse BLA-projecting IL neurons. Front. Neurosci. 19:1532078

Lopez GC, Lerner TN. 2025. How Dopamine Enables Learning from Aversion. Curr. Opin. Behav. Sci. 61:

Lutas A, Fernando K, Zhang SX, Sambangi A, Andermann ML. 2022. History-dependent dopamine release increases cAMP levels in most basal amygdala glutamatergic neurons to control learning. Cell Rep. 38(4):110297

Lutas A, Kucukdereli H, Alturkistani O, Carty C, Sugden AU, et al. 2019. State-specific gating of salient cues by midbrain dopaminergic input to basal amygdala. Nat. Neurosci. 22(11):1820–33

Maren S. 2005. Synaptic mechanisms of associative memory in the amygdala. Neuron. 47(6):783–86

Margolis EB, Lock H, Hjelmstad GO, Fields HL. 2006. The ventral tegmental area revisited: is there an electrophysiological marker for dopaminergic neurons? J Physiol (Lond). 577(Pt 3):907–24

Mathis A, Mamidanna P, Cury KM, Abe T, Murthy VN, et al. 2018. DeepLabCut: markerless pose estimation of user-defined body parts with deep learning. Nat. Neurosci. 21(9):1281–89

McCutcheon JE, Ebner SR, Loriaux AL, Roitman MF. 2012. Encoding of aversion by dopamine and the nucleus accumbens. Front. Neurosci. 6:137

McGarry LM, Carter AG. 2017. Prefrontal cortex drives distinct projection neurons in the basolateral amygdala. Cell Rep. 21(6):1426–33

Mingote S, Chuhma N, Kusnoor SV, Field B, Deutch AY, Rayport S. 2015. Functional connectome analysis of dopamine neuron glutamatergic connections in forebrain regions. J. Neurosci. 35(49):16259–71

Morales M, Margolis EB. 2017. Ventral tegmental area: cellular heterogeneity, connectivity and behaviour. Nat. Rev. Neurosci. 18(2):73–85

Morishita Y, Fuentes I, Gonzalez-Salinas S, Favate J, Mejaes J, et al. 2024. Dopamine release and dopamine-related gene expression in the amygdala are modulated by the gastrin-releasing peptide in opposite directions during stress-enhanced fear learning and extinction. Mol. Psychiatry

Muller JF, Mascagni F, McDonald AJ. 2009. Dopaminergic innervation of pyramidal cells in the rat basolateral amygdala. Brain Struct. Funct. 213(3):275–88

Namburi P, Beyeler A, Yorozu S, Calhoon GG, Halbert SA, et al. 2015. A circuit mechanism for differentiating positive and negative associations. Nature. 520(7549):675–78

Ng KH, Pollock MW, Urbanczyk PJ, Sangha S. 2018. Altering D1 receptor activity in the basolateral amygdala impairs fear suppression during a safety cue. Neurobiol. Learn. Mem. 147:26–34

O'Neill P-K, Gore F, Salzman CD. 2018. Basolateral amygdala circuitry in positive and negative valence. Curr. Opin. Neurobiol. 49:175–83

Oleson EB, Gentry RN, Chioma VC, Cheer JF. 2012. Subsecond dopamine release in the nucleus accumbens predicts conditioned punishment and its successful avoidance. J. Neurosci. 32(42):14804–8

Orsini CA, Willis ML, Gilbert RJ, Bizon JL, Setlow B. 2016. Sex differences in a rat model of risky decision making. Behav. Neurosci. 130(1):50–61

Ottenheimer DJ, Vitale KR, Ambroggi F, Janak PH, Saunders BT. 2024. Orbitofrontal Cortex Mediates Sustained Basolateral Amygdala Encoding of Cued Reward-Seeking States. J. Neurosci. 44(46):

Park J, Moghaddam B. 2017. Risk of punishment influences discrete and coordinated encoding of reward-guided actions by prefrontal cortex and VTA neurons. eLife. 6:

Paton JJ, Belova MA, Morrison SE, Salzman CD. 2006. The primate amygdala represents the positive and negative value of visual stimuli during learning. Nature. 439(7078):865–70

Patriarchi T, Cho JR, Merten K, Howe MW, Marley A, et al. 2018. Ultrafast neuronal imaging of dopamine dynamics with designed genetically encoded sensors. Science. 360(6396):

Pinard CR, Muller JF, Mascagni F, McDonald AJ. 2008. Dopaminergic innervation of interneurons in the rat basolateral amygdala. Neuroscience. 157(4):850–63

Poulin J-F, Caronia G, Hofer C, Cui Q, Helm B, et al. 2018. Mapping projections of molecularly defined dopamine neuron subtypes using intersectional genetic approaches. Nat. Neurosci. 21(9):1260–71

Revay R, Vaughan R, Grant S, Kuhar MJ. 1996. Dopamine transporter immunohistochemistry in median eminence, amygdala, and other areas of the rat brain. Synapse

Rogan MT, Leon KS, Perez DL, Kandel ER. 2005. Distinct neural signatures for safety and danger in the amygdala and striatum of the mouse. Neuron. 46(2):309–20

Roitman MF, Wheeler RA, Wightman RM, Carelli RM. 2008. Real-time chemical responses in the nucleus accumbens differentiate rewarding and aversive stimuli. Nat. Neurosci. 11(12):1376–77

Saddoris MP, Gallagher M, Schoenbaum G. 2005. Rapid associative encoding in basolateral amygdala depends on connections with orbitofrontal cortex. Neuron. 46(2):321–31

Sangha S, Chadick JZ, Janak PH. 2013. Safety encoding in the basal amygdala. J. Neurosci. 33(9):3744–51

Sangha S, Diehl MM, Bergstrom HC, Drew MR. 2020. Know safety, no fear. Neurosci. Biobehav. Rev. 108:218–30

Sangha S. 2015. Plasticity of fear and safety neurons of the amygdala in response to fear extinction. Front. Behav. Neurosci. 9:354

Saunders BT, Richard JM, Margolis EB, Janak PH. 2018. Dopamine neurons create Pavlovian conditioned stimuli with circuit-defined motivational properties. Nat. Neurosci. 21(8):1072–83

Schultz W. 2016. Dopamine reward prediction-error signalling: a two-component response. Nat. Rev. Neurosci. 17(3):183–95

Scibilia RJ, Lachowicz JE, Kilts CD. 1992. Topographic nonoverlapping distribution of D1 and D2 dopamine receptors in the amygdaloid nuclear complex of the rat brain. Synapse. 11(2):146–54

Sengupta A, Yau JOY, Jean-Richard-Dit-Bressel P, Liu Y, Millan EZ, et al. 2018. Basolateral amygdala neurons maintain aversive emotional salience. J. Neurosci. 38(12):3001–12

Sias AC, Jafar Y, Goodpaster CM, Ramírez-Armenta K, Wrenn TM, et al. 2024. Dopamine projections to the basolateral amygdala drive the encoding of identity-specific reward memories. Nat. Neurosci. 27(4):728–36

Sias AC, Morse AK, Wang S, Greenfield VY, Goodpaster CM, et al. 2021. A bidirectional corticoamygdala circuit for the encoding and retrieval of detailed reward memories. eLife. 10:

Steinberg EE, Boivin JR, Saunders BT, Witten IB, Deisseroth K, Janak PH. 2014. Positive reinforcement mediated by mid-

brain dopamine neurons requires D1 and D2 receptor activation in the nucleus accumbens. PLoS ONE. 9(4):e94771

Stuber GD, Sparta DR, Stamatakis AM, van Leeuwen WA, Hardjoprajitno JE, et al. 2011. Excitatory transmission from the amygdala to nucleus accumbens facilitates reward seeking. Nature. 475(7356):377–80

Takahashi H, Takano H, Kodaka F, Arakawa R, Yamada M, et al. 2010. Contribution of dopamine D1 and D2 receptors to amygdala activity in human. J. Neurosci. 30(8):3043–47

Tang W, Kochubey O, Kintscher M, Schneggenburger R. 2020. A VTA to Basal Amygdala Dopamine Projection Contributes to Signal Salient Somatosensory Events during Fear Learning. J. Neurosci. 40(20):3969–80

Tye KM, Janak PH. 2007. Amygdala neurons differentially encode motivation and reinforcement. J. Neurosci. 27(15):3937–45

Tye KM, Stuber GD, de Ridder B, Bonci A, Janak PH. 2008. Rapid strengthening of thalamo-amygdala synapses mediates cue-reward learning. Nature. 453(7199):1253–57

Tye KM, Tye LD, Cone JJ, Hekkelman EF, Janak PH, Bonci A. 2010. Methylphenidate facilitates learning-induced amygdala plasticity. Nat. Neurosci. 13(4):475–81

van Elzelingen W, Goedhoop J, Warnaar P, Denys D, Arbab T, Willuhn I. 2022a. A unidirectional but not uniform striatal landscape of dopamine signaling for motivational stimuli. Proc Natl Acad Sci USA. 119(21):e2117270119

van Elzelingen W, Warnaar P, Matos J, Bastet W, Jonkman R, et al. 2022b. Striatal dopamine signals are region specific and temporally stable across action-sequence habit formation. Curr. Biol. 32(5):1163-1174.e6

Wheeler A-R, Truckenbrod LM, Boehnke A, Kahanek P, Orsini CA. 2024. Sex differences in sensitivity to dopamine receptor manipulations of risk-based decision making in rats. Neuropsychopharmacology. 49(13):1978–88

Whitelaw RB, Robbins TW, Everitt BJ, Markou A. 1996. Excitotoxic lesions of the basolateral amygdala impair the acquisition of cocaine-seeking behaviour under a second-order schedule of reinforcement. Psychopharmacology. 127(3):213–24

Witten IB, Steinberg EE, Lee SY, Davidson TJ, Zalocusky KA, et al. 2011. Recombinase-driver rat lines: tools, techniques, and optogenetic application to dopamine-mediated reinforcement. Neuron. 72(5):721–33

Wojick JA, Paranjapye A, Chiu JK, Mahmood M, Oswell C, et al. 2024. A nociceptive amygdala-striatal pathway for chronic pain aversion. BioRxiv

Wolff AR, Saunders BT. 2024. Sensory cues potentiate VTA dopamine mediated reinforcement. eNeuro. 11(2):

Yang H, de Jong JW, Tak Y, Peck J, Bateup HS, Lammel S. 2018. Nucleus accumbens subnuclei regulate motivated behavior via direct inhibition and disinhibition of VTA dopamine subpopulations. Neuron. 97(2):434-449.e4

Yokota S, Suzuki Y, Hamami K, Harada A, Komai S. 2017. Sex differences in avoidance behavior after perceiving potential risk in mice. Behav. Brain Funct. 13(1):9

Zhang X, Guan W, Yang T, Furlan A, Xiao X, et al. 2021. Genetically identified amygdala-striatal circuits for valence-specific behaviors. Nat. Neurosci. 24(11):1586–1600

Zhang X, Li B. 2018. Population coding of valence in the basolateral amygdala. Nat. Commun. 9(1):5195

Zhao Q, Ito T, Soko C, Hori Y, Furuyama T, et al. 2022. Histochemical Characterization of the Dorsal Raphe-Periaqueductal Grey Dopamine Transporter Neurons Projecting to the Extended Amygdala. eNeuro. 9(3): ENEURO.0121-22.2022

Supplemental Material

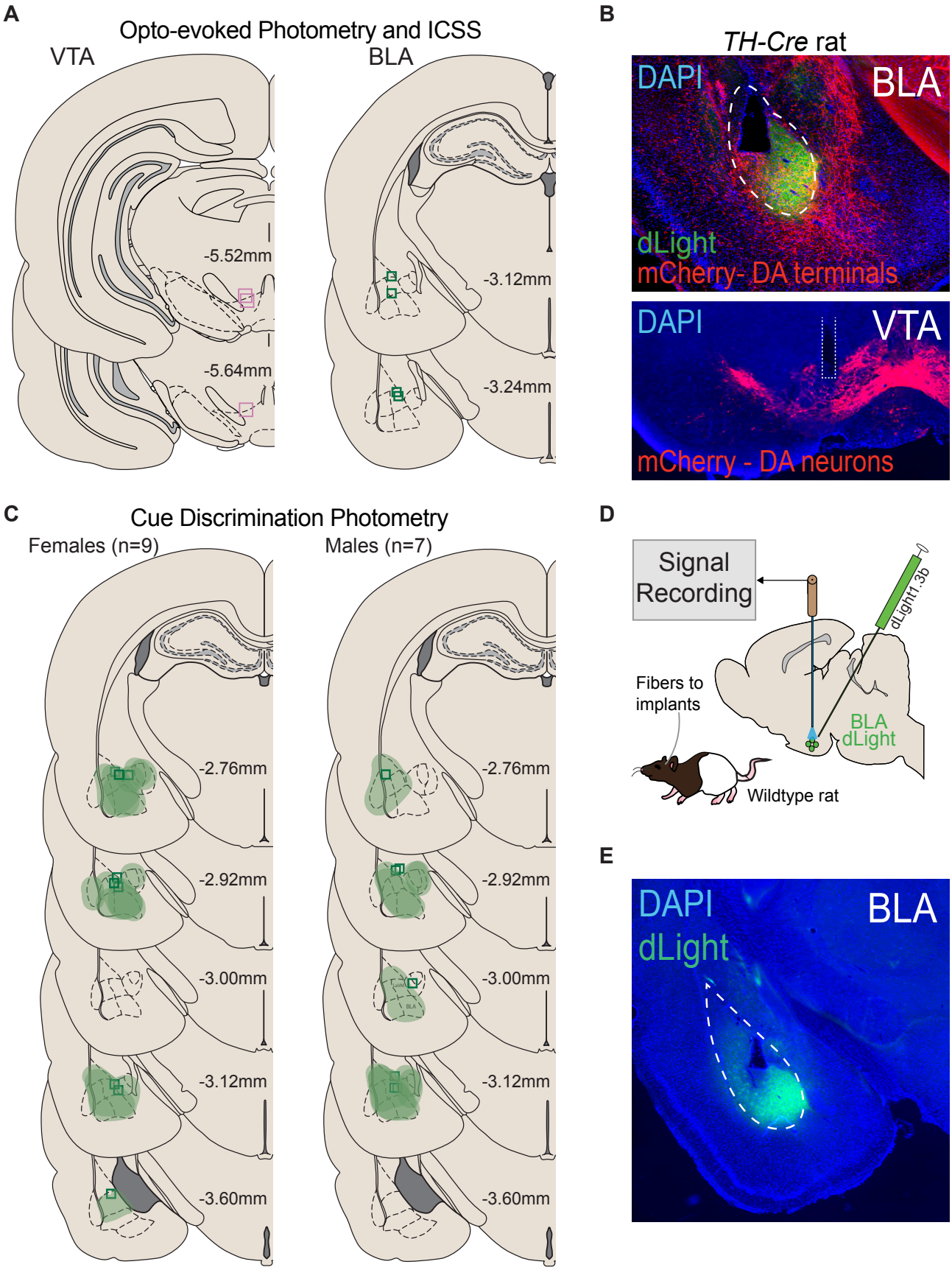

Fig S1 | Histology for VTA-BLA optogenetic stimulation and dLight fiber photometry recordings

A) Optic fiber placements for rats used to measure optogenetically-evoked dopamine signals and ICSS behavior following optogenetic activation of VTA dopamine terminals in the BLA. B) Histology images showing BLA dopamine terminals (top) and VTA dopamine neuron cell bodies (bottom) expressing mCherry from a cre-dependent viral injection in the VTA of TH-cre rats. C) dLight 1.3b viral spread and optic fiber placements for the photometry cue discrimination experiments in female (n=9) and B) male (n=7) rats. D) Schematic of the fiber photometry approach with the dopamine sensor, dLight 1.3b, expressed in the BLA of freely moving rats. E) Representative image of dLight virus expression in the BLA.

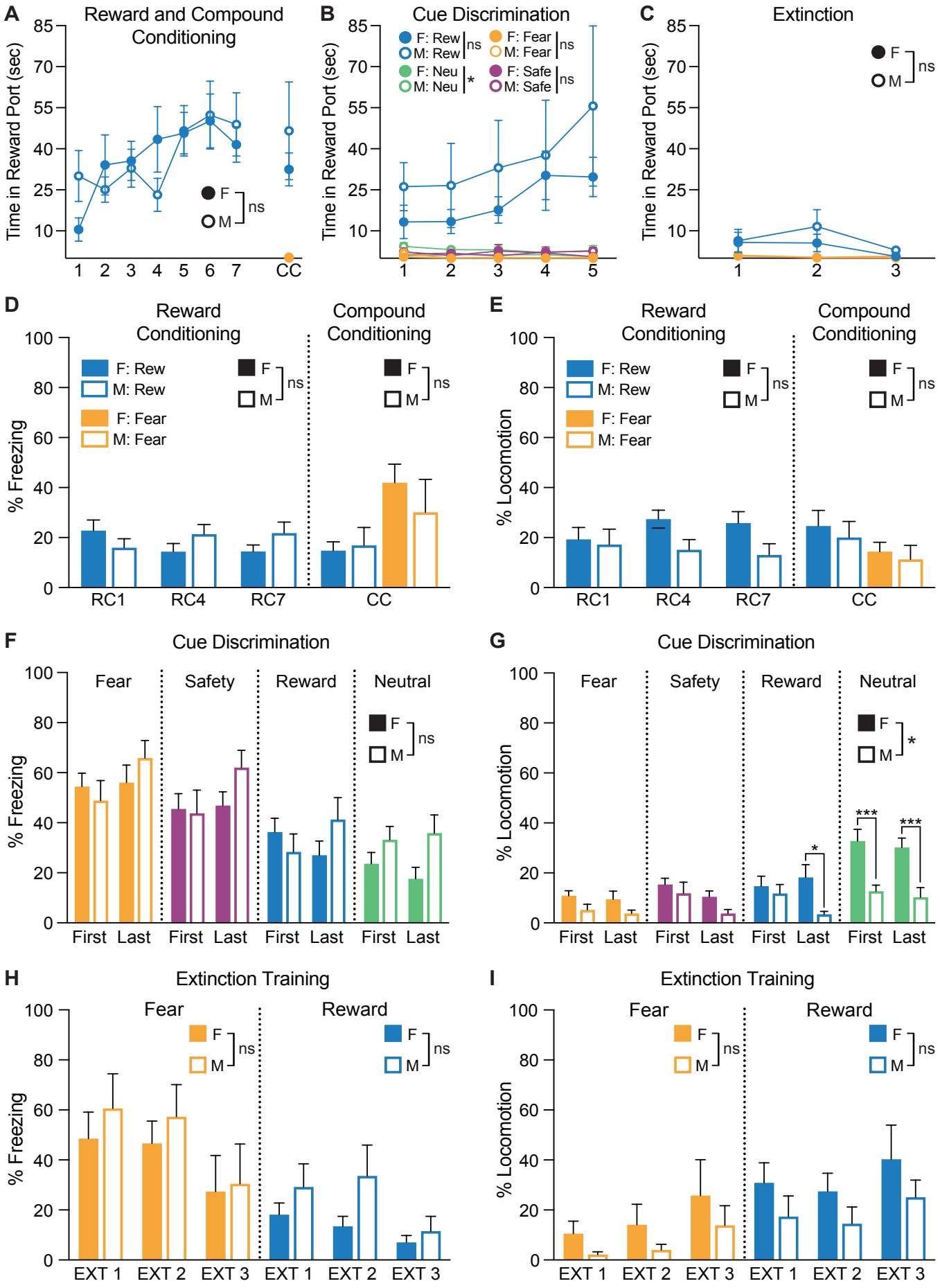
A
Reward and Compound Conditioning
Time in Reward Port (sec)
F
M
ns
1 2 3 4 5 6 7 CC
B
Cue Discrimination
F: Rew
M: Rew
ns
F: Fear
M: Fear
ns
F: Neu
M: Neu
*
F: Safe
M: Safe
ns
1 2 3 4 5
C
Extinction
F
M
ns
1 2 3
D
Reward Conditioning
Compound Conditioning
% Freezing
F: Rew
M: Rew
F: Fear
M: Fear
F
M
ns
RC1 RC4 RC7 CC
E
Reward Conditioning
Compound Conditioning
% Locomotion
RC1 RC4 RC7 CC
F
Cue Discrimination
Fear
Safety
Reward
Neutral
% Freezing
First Last First Last First Last First Last
G
Cue Discrimination
% Locomotion
*
***
***
H
Extinction Training
Fear
Reward
% Freezing
EXT 1 EXT 2 EXT 3 EXT 1 EXT 2 EXT 3
I
Extinction Training
% Locomotion

Fig S2 | Reward and threat-related behaviors do not systematically vary by sex

A) Time spent in the sucrose port split between females (n=9; filled) and males (n=7; open) across reward conditioning and compound conditioning. There was no sex difference in port entry behaviors during the reward cue presentations ($F(1,14)=7.964e-006$, $p=0.9978$) nor the fear cue presentations ($t(7)=1.617$, $p=0.1498$) in early training phases. B) Time spent in the sucrose port for all cue types during cue discrimination training for females (filled circles) and males (open circles). There were no differences in time spent in port during reward cue ($F(1,14)=0.9062$, $p=0.3573$), fear cue ($F(1,14)=1.350$, $p=0.2495$), or safety cue ($F(1,14)=1.350$, $p=0.001605$) presentations. However, there was a mildly significant main effect of sex for neutral cue presentations ($F(1,14)=4.950$, $p=0.0431$), where males typically spent more time in the port. C) During extinction training, females and males spent equivalent time in the sucrose port during reward cue ($F(1,14)=0.1738$, $p=0.6839$) and fear cue ($F(1,14)=0.4873$, $p=0.4966$) presentations. D) Percent of time freezing during cue presentations was not significantly different between females and males for either cue type during reward conditioning ($F(1,14)=0.3191$, $p=0.5811$) and compound conditioning ($F(1,7)=0.2314$, $p=0.6452$). E) Percent of time locomoting during cue presentations was not significantly different between the sexes for either cue type during reward conditioning ($F(1,14)=2.283$, $p=0.1530$) and compound conditioning ($F(1,7)=0.3095$, $p=0.5953$). F) There were no significant differences in freezing behavior between males and females for any cue type during the first ($F(1,14)=0.01308$, $p=0.9106$) or last ($F(1,14)=4.154$, $p=0.0609$) day of the cue discrimination phase. G) When comparing locomotion to cue types during the first cue discrimination session, locomotion was modulated by cue type ($F(3,42)=9.508$, $p<0.0001$) and sex ($F(1,14)=5.352$, $p=0.0364$). Further, different cues prompted different levels of locomotion between females and males (cue type x sex interaction, $F(3,42)=4.169$, $p=0.0113$), especially during the neutral cue, where females locomote more during these presentations ($p=0.0005$). Locomotion during the final cue discrimination session was also modulated by cue type ($F(3,42)=12.32$, $p<0.0001$) and sex ($F(1,14)=11.22$, $p=0.0048$). Cues also prompted different levels of locomotion between females and males (cue type x sex interaction, $F(3,42)=3.530$, $p=0.0228$), specifically during the neutral ($p=0.0003$) and reward cues ($p=0.0108$), where females locomote more during these presentations. H) Cue-evoked freezing behaviors did not differ between females and males during extinction training during fear cue ($F(1,14)=0.4042$, $p=0.5352$) or reward cue ($F(1,14)=2.423$, $p=0.1419$) presentations. I) Cue-evoked locomotion behaviors did not differ between females and males during extinction training during fear cue ($F(1,14)=0.9850$, $p=0.3378$) or reward cue ($F(1,14)=1.640$, $p=0.2211$) presentations. Data represent mean ± SEM. *p<0.05, *p<0.01, ***p<0.001.

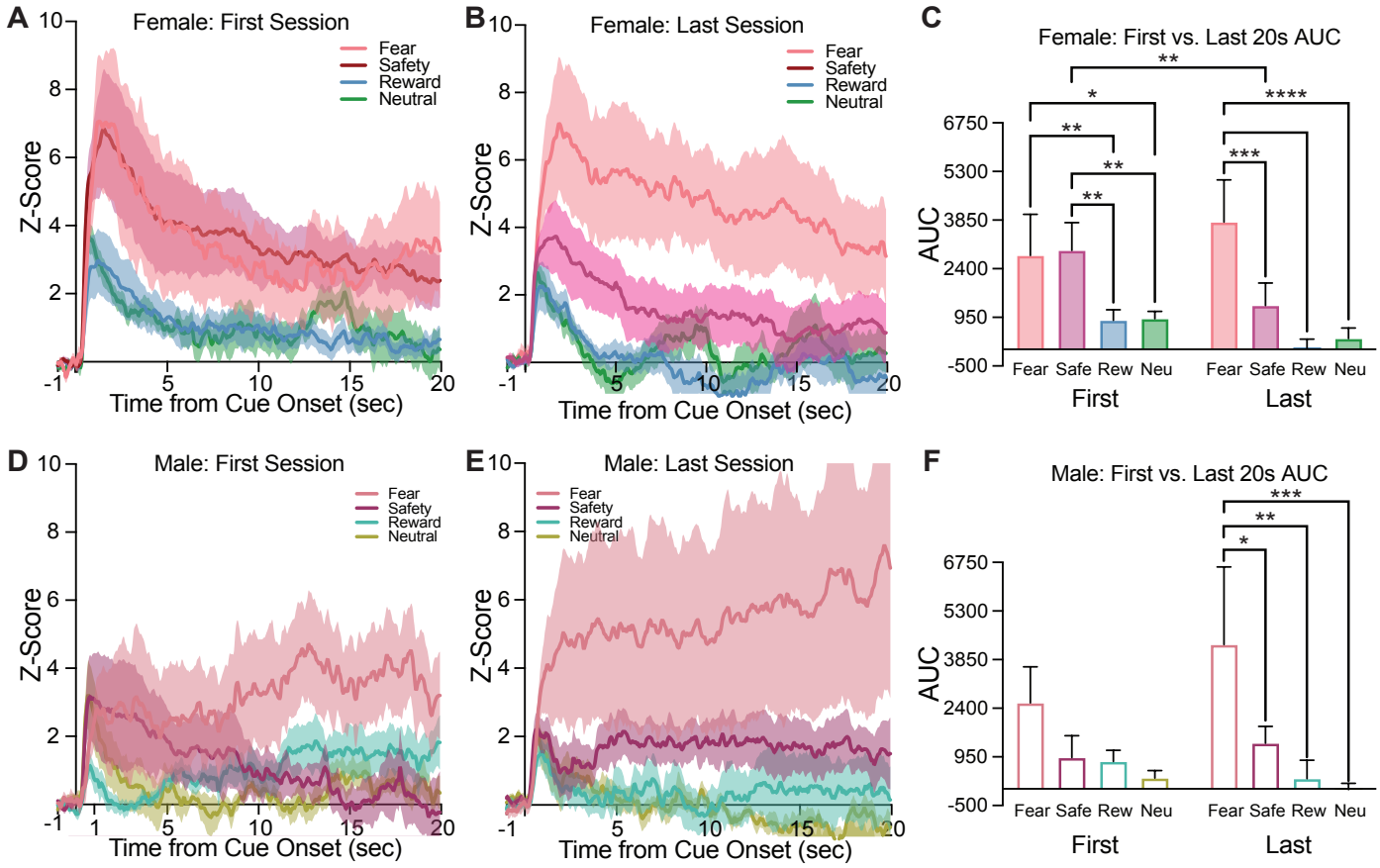

Fig S3 | Fear and safety cues prompt larger and more sustained dopamine compared to the reward and neutral cues in both males and females during cue discrimination

A) In females (n=9), on the first discrimination session all four cue types elicited a positive peak and remained above baseline for the full 20s cue presentation. Specifically, the fear and safety cues prompted larger, more sustained BLA dopamine traces compared to the reward and neutral cues. B) During the last discrimination session, BLA dopamine release in females remained highly sustained for the full 20s fear cue periods, while the dopamine release to the reward and neutral cues returned to baseline around 5s. The safety cue BLA dopamine trace had an intermediate magnitude and remained moderately sustained throughout the entire 20s presentation. C) AUC measures of female BLA dopamine signals show cue-induced dopamine was modulated by cue type ($F(3,24)=5.019$, $p=0.0077$) and this modulation changed across sessions (session x cue type interaction $F(3,24)=3.949$, $p=0.0202$). In the first discrimination session the fear cue trace is significantly larger than the reward ($p=0.0099$) and neutral ($p=0.0122$) cue traces, while the safety cue trace is also significantly larger than the reward ($p=0.0051$) and neutral ($p=0.0064$) cue traces. The amount of safety cue evoked dopamine significantly decreased between the first and last cue discrimination sessions ($p=0.0070$). D) In males (n=7), all four cue types prompt increases in BLA dopamine during the first discrimination session. Qualitatively, the fear cue is more elevated throughout the 20-s cue presentation compared to the other cue types. E) Male BLA dopamine during the last discrimination session showed the fear-evoked trace remained elevated for the full 20-s period. The reward and neutral cues returned to baseline around 5s, while the safety cue serves as an intermediary signal in terms of magnitude and elevation. F) AUC measures of male BLA dopamine signals reveal cue-induced dopamine was modulated by cue type ($F(3,18)=4.813$, $p=0.0124$). On the last discrimination session, only the fear cue elicited significantly larger dopamine transmission compared to all other cue types (safety: $p=0.0196$; reward: $p=0.0016$; neutral: $p=0.0007$). Data represent mean ± SEM. *$p<0.05$, **$p<0.01$, ***$p<0.001$, ****$p<0.0001$.